

Proteomic and physiological responses of leopard sharks (*Triakis semifasciata*) to salinity change

W. W. Dowd^{1,2,*}, B. N. Harris³, J. J. Cech, Jr² and D. Kültz¹

¹Physiological Genomics Group, Department of Animal Science and ²Department of Wildlife, Fish, and Conservation Biology, University of California, Davis, 1 Shields Avenue, Davis, CA 95616, USA and ³Department of Biology, 3386 Spieth Hall, University of California, Riverside, CA 92521, USA

*Author for correspondence at present address: Hopkins Marine Station of Stanford University, Pacific Grove, CA 93950, USA (wwdowd@stanford.edu)

Accepted 14 September 2009

SUMMARY

Partially euryhaline elasmobranchs may tolerate physiologically challenging, variable salinity conditions in estuaries as a trade-off to reduce predation risk or to gain access to abundant food resources. To further understand these trade-offs and to evaluate the underlying mechanisms, we examined the responses of juvenile leopard sharks to salinity changes using a suite of measurements at multiple organizational levels: gill and rectal gland proteomes (using 2-D gel electrophoresis and tandem mass spectrometry), tissue biochemistry (Na⁺/K⁺-ATPase, caspase 3/7 and chymotrypsin-like proteasome activities), organismal physiology (hematology, plasma composition, muscle moisture) and individual behavior. Our proteomics results reveal coordinated molecular responses to low salinity – several of which are common to both rectal gland and gill – including changes in amino acid and inositol (i.e. osmolyte) metabolism, energy metabolism and proteins related to transcription, translation and protein degradation. Overall, leopard sharks employ a strategy of maintaining plasma urea, ion concentrations and Na⁺/K⁺-ATPase activities in the short-term, possibly because they rarely spend extended periods in low salinity conditions in the wild, but the sharks osmoconform to the surrounding conditions by 3 weeks. We found no evidence of apoptosis at the time points tested, while both tissues exhibited proteomic changes related to the cytoskeleton, suggesting that leopard sharks remodel existing osmoregulatory epithelial cells and activate physiological acclimatory responses to solve the problems posed by low salinity exposure. The behavioral measurements reveal increased activity in the lowest salinity in the short-term, while activity decreased in the lowest salinity in the long-term. Our data suggest that physiological/behavioral trade-offs are involved in using estuarine habitats, and pathway modeling implicates tumor necrosis factor α (TNF α) as a key node of the elasmobranch hyposmotic response network.

Supplementary material available online at <http://jeb.biologists.org/cgi/content/full/213/2/210/DC1>

Key words: elasmobranch, osmoregulation, urea, Na⁺/K⁺-ATPase, focal animal sampling, proteomics, MALDI-TOF-TOF mass spectrometry, pathway analysis, tumor necrosis factor.

INTRODUCTION

Salinity change is an important environmental challenge faced by estuarine and coastal fishes, which have evolved a suite of morphological, physiological and behavioral characteristics for coping with such environmental variability. Species of the subclass Elasmobranchii (the sharks, skates and rays) commonly utilize coastal and estuarine habitats, particularly at certain times of the year or specific life-history stages (e.g. juvenile nursery areas) (Heupel et al., 2007; Springer, 1967). However, with relatively few exceptions, most elasmobranchs exhibit low tolerance of salinity change – the majority being stenohaline (some in freshwater) or partially euryhaline. From a physiological perspective, partially euryhaline elasmobranchs entering estuaries with variable salinity may incur significant costs due to their urea-based osmoregulatory strategy, which creates slightly hyperosmotic or isosmotic conditions within the shark relative to full-strength seawater (SW) (Evans et al., 2004; Hazon et al., 2003). From an ecological perspective, elasmobranchs in estuaries, particularly juveniles, may enjoy the benefits of abundant food resources as well as spatial refuge from larger predators found in the oceans (Branstetter, 1990; Heupel et al., 2007). In order to better understand the potential trade-offs involved in using such dynamic, potentially stressful habitats, we

need to determine whether (i) the animals are simply tolerating challenging salinity conditions in exchange for greater net benefits, (ii) they are capable of coping physiologically with those conditions, or (iii) they employ other options such as behavioral avoidance (e.g. moving away from low/changing salinity areas of the estuary) or behavioral modulation (e.g. reducing activity to conserve energy for physiological acclimation when avoidance is not possible) to compensate for physiological ‘shortcomings’. Such diverse possibilities highlight the need for an integrative approach to answer questions in ecological physiology, incorporating techniques that provide insight into responses at different levels of biological organization (i.e. from individual cells to whole organisms).

At the molecular level, we have previously applied 2-D gel electrophoresis and mass spectrometry-based proteomics techniques to understand the adjustments made in fish tissues to physiological challenges (Dowd et al., 2008; Kültz et al., 2007). Proteins are the primary executioners of cell functions, and the proteome integrates changes in gene expression, mRNA stability and protein post-translational modification and turnover in response to environmental change (Kültz, 2005). Gel-based proteomics, like cDNA microarrays and other ‘omics’ approaches, is a powerful tool for generating new mechanistic hypotheses that then can be tested by other means (e.g.

Matey et al., 2009). However, very few studies have attempted to integrate proteomics with other levels of biological organization in ecologically relevant scenarios for 'non-model' organisms. Due to the unique osmoregulatory strategy of elasmobranchs and their basal position in the vertebrate phylogeny, unraveling the key players in their osmoregulatory response mechanisms will provide both evolutionary and ecological insights.

In this study, we exposed leopard sharks (*Triakis semifasciata* Girard 1855) to salinity changes representative of those likely to be encountered in estuaries in order to assess their responses from the molecular level through to the organismal level. Sharks provide abundant tissue for proteomics and biochemistry, and they are amenable to complementary techniques at the organismal level. Leopard sharks inhabit California estuaries at all times of year, where they can experience salinity changes on several time scales (Fig. 1), including stochastic changes due to extreme rainfall events or anthropogenic activities. These salinity changes can be fairly rapid, leading to shifts of as much as 18 parts per thousand (p.p.t.) in just 12 h. Leopard sharks have been captured in San Francisco Bay at salinities as low as 14 p.p.t. but they are more commonly encountered at salinities greater than 18 p.p.t. (J. Diesel, Marine Science Institute, personal communication). These data suggest a lower physiological tolerance threshold (i.e. leopard sharks are partially euryhaline) and/or behavioral avoidance of lower salinities in the wild.

Because responses to environmental challenges are likely to vary among tissues, depending on both their exposure to surrounding conditions and their functions, we assessed salinity-dependent changes in both the rectal gland and gill proteomes. The mechanisms of salt secretion in the elasmobranch rectal gland have been thoroughly described (reviewed in Evans et al., 2004), yet we know little about how these functions are modulated by environmental change or how other aspects of the cellular response are integrated with higher levels of organization. The elasmobranch gill (the principal semi-permeable interface between water of changing salinity and the internal milieu) is thought to play a relatively limited role in seawater osmoregulatory processes aside from acting as a barrier to urea loss [but see Evans et al. (Evans et al., 2004) for a review of the gill's putative function in freshwater elasmobranchs]. Using proteomics and physiological data in concert with laboratory measurements of behavior, we discuss mechanisms and propose novel key regulators in the elasmobranch osmoregulatory response network. These mechanisms may underlie the trade-offs that influence estuarine habitat use.

MATERIALS AND METHODS

Animal collection, maintenance and salinity control

Experiments were carried out at the Bodega Marine Laboratory, CA, USA, during June–August 2005 (experiments 1 and 2) and May 2007 (experiment 3). Leopard sharks ($N=45$) were collected in Bodega Harbor using a beach seine and transported in coolers containing oxygenated seawater to the laboratory. There they were held in a 3.7 m diameter, flow-through tank at natural photoperiod

for 2–62 days prior to the beginning of an experiment (2005: 33.4 ± 0.1 p.p.t., $13.5 \pm 0.2^\circ\text{C}$, 7.31 ± 0.13 mg l⁻¹ dissolved oxygen; 2007: 33.8 ± 0.1 p.p.t., $10.7 \pm 0.2^\circ\text{C}$, 7.69 ± 0.07 mg l⁻¹). Sharks were fed *ad libitum* rations of squid (*Loligo* spp.) and/or Bay ghost shrimp (*Neotrypaea californiensis* Dana 1854) in the holding tank.

Salinity experiments were conducted in flow-through 1600–1900 liter fiberglass tanks by varying the ratio of inflowing seawater (SW; ~34 p.p.t.) to freshwater (FW; 2.9 p.p.t.) to each tank using two in-line flow meters. The water turnover rate in the experimental tanks was 32–45% per hour (h). Salinity was reduced gradually from full-strength SW (experiments 1 and 2 over 18 h; experiment 3 over 11 h) in order to mimic rates of salinity change likely to be experienced by sharks in the wild. To avoid stress from aerial exposure, all movements between tanks were performed using a watertight sling. All procedures were approved by the University of California, Davis IACUC (Protocols 11745 and 12746).

Experiment 1: Short-term (48 h) osmoregulatory responses to salinity change

Sharks in this experiment were subjected to short-term (~48 h) exposures to one of three salinity treatments: 33.3 p.p.t. (100% SW control), 27.6 p.p.t. (80% SW) or 20.7 p.p.t. (60% SW) [$N=18$; 1245 ± 101 g; 68.5 ± 2.1 cm total length (TL)]. Prior to the experiment, 12 of these sharks were anesthetized in Fiquel™ MS-222 (Argent Chemical Laboratories, Redmond, WA, USA) and cannulated *via* the caudal artery with a 1.5 m length of PE50 tubing using a 17G Touhy needle to allow repeated blood sampling during the experiment (Hopkins and Cech, 1995). The cannula was filled with heparinized elasmobranch Ringer solution (Anderson et al., 2002). During this short procedure each shark was weighed, sexed, measured and photographed for identification. Sharks were allowed to recover in 100% SW in the experimental tanks for 44–68 h prior to salinity change. Sham surgeries were conducted on the remaining six sharks; the procedure was identical to that for cannulated animals, except the cannula was never inserted. The sharks were not fed during the recovery period or during the experiment.

At the start of the experiment (time=0 h), an initial blood sample (~0.6–0.7 ml) was drawn through the cannula while all sharks remained at 100% SW. Salinity change commenced 6 h thereafter, and repeated blood samples were collected at 12 h (during salinity change), 24 h (immediately after salinity change) and 48 h. Water samples were collected at each time point for comparison with the blood plasma. Sharks were euthanized in ice-cold seawater by pithing at 53–54 h and were immediately weighed and measured.

Experiment 2: Long-term (3 weeks) osmoregulatory and tissue responses to salinity change

The sharks in this experiment ($N=9$; 2241 ± 526 g, 81.5 ± 5.5 cm TL) were exposed to the same salinity treatments (100%, 80% and 60% SW) and rates of salinity change as those in experiment 1, but they remained at the final salinity for 3 weeks. Prior to the experiment, each shark was lightly anesthetized in MS-222 and then weighed,

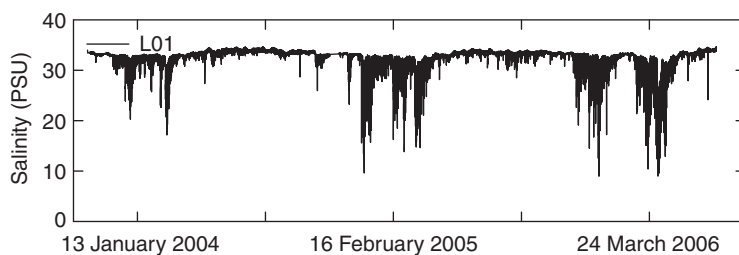


Fig. 1. Long-term salinity record for a single monitoring station in Elkhorn Slough, a California estuary inhabited by leopard sharks, demonstrating interannual, seasonal, and shorter scale (e.g. tidal) salinity variability. Data obtained from the Monterey Bay Aquarium Research Institute's Land Ocean Biogeochemical Observatory database (www.mbari.org/lobo/).

sexed, measured and photographed for identification. The sharks were then allowed 48 h to recover from handling in 100% SW before commencing the salinity change. These sharks were not cannulated, because the cannulae tend to clot within 3–4 days. The sharks were fed a controlled daily ration of squid (~2% body mass per day).

At the end of the experiment a blood sample was drawn from the caudal artery, and sharks were then euthanized as in experiment 1. In order to clear the body of background red blood cells (RBC) for biochemistry and proteomics, we perfused the animal *via* the heart with elasmobranch Ringer solution and the sinus venosus was severed to allow exsanguination for several minutes after the gills turned white. Following perfusion, we collected gill (second left arch), rectal gland and kidney (just anterior to mid-point). Two replicates of each tissue were snap-frozen in liquid nitrogen and then stored at -80°C until analysis.

Experiment 3: Short-term (24 h) osmoregulatory and tissue responses to salinity change

In this experiment, 17 sharks (1668 ± 130 g, 74.8 ± 2.0 cm TL) were exposed to gradual changes in salinity from 100% SW to 100% SW (control, $N=5$), 75% SW ($N=6$) and 50% SW ($N=6$). After 24 h, the sharks were euthanized and perfused as above, and then blood and tissues were collected in duplicate as in experiment 2.

Hematological, plasma and tissue analyses

Hematology

Heparinized blood samples were collected in microfuge tubes and stored on ice until analysis (<1 h). We determined hematocrit (HCT; % packed red blood cells) using heparinized hematocrit tubules. In experiment 1 only, we determined RBC count (10^5 cells per mm^3) using diluting pipettes and hemocytometers on a $\times 40$ objective light microscope (Cooper and Morris, 1998). Using these data, we calculated mean corpuscular volume (MCV).

Plasma constituents

Blood samples were centrifuged at $5000g$ for 5 min, and the plasma was removed and frozen before analysis. Plasma samples were analyzed in triplicate for Na^+ and K^+ concentrations (mmol l^{-1}) by flame photometry (Instrumentation Laboratory 343, Bedford, MA, USA), Cl^- concentration (mmol l^{-1}) using a chloride titrator (Radiometer CMT10, Copenhagen, Denmark; or Labconco Digital Chloridometer, Kansas City, MO, USA), and osmolality (mOsmol kg^{-1}) using a vapor pressure osmometer (Wescor VaproTM 5520, Logan, UT, USA). Plasma urea concentration (mmol l^{-1}) was determined spectrophotometrically using a biological urea nitrogen kit (Randox Laboratories, Crumlin, UK) modified for use on a microplate reader. Total plasma protein concentration (g%) was measured by refractometry.

Tissue measurements

At the conclusion of all three experiments we collected 2–3 g of epaxial white muscle (ventral to the second dorsal fin) in duplicate. White muscle tissues were then dried to constant mass at 55°C to determine the percentage muscle moisture. In experiments 1 and 2 the rectal gland and liver were excised and weighed to assess the relationships of rectal gland mass and liver mass to body mass.

Proteomics

2-D gel electrophoresis and image analysis

Proteins regulated by exposure to salinity change in the leopard shark rectal gland and gill were identified using 2-D gel electrophoresis and tandem mass spectrometry (MS) following the methods of Dowd

et al. (Dowd et al., 2008). Based on the results of our physiological measurements in experiment 1, we selected the 24 h time point as being representative of the most physiologically challenging (i.e. largest osmotic gradient between shark and environment) conditions faced during the short-term experiment. Proteomics analyses were carried out on tissues from the same individuals used in experiment 3 ($N=5$ or 6 per treatment for rectal gland; $N=3$ for gill for 50% and 100% SW), with separate gels run for each individual and each tissue. Briefly, proteins were extracted, precipitated in acetone with 10% trichloroacetic acid, loaded (1 mg per sample) onto 18 cm immobilized pH 3–10 non-linear gradient strips by passive overnight rehydration, separated in the first dimension by isoelectric focusing, equilibrated with dithiothreitol and iodoacetamide, and then run on 16 cm second dimension SDS-PAGE gels (Dowd et al., 2008; Valkova et al., 2005). 2-D gels were fixed and stained with Coomassie Brilliant Blue G250, destained in purified water and then scanned for densitometry. The individual gel images were aligned, fused into a master gel image for each tissue and quantified based on the normalized volume of each spot (relative to the total volume of all spots) using Delta 2D software (v3.6, Decodon, Germany) (Dowd et al., 2008). Protein spots whose abundance changed significantly [$P < 0.05$; expression ratio > 2 (increased by $> 100\%$) or < 0.5 (decreased by $> 50\%$)] between treatments were excised and processed for MS identification.

MS and bioinformatics database searches

Protein spots of interest were digested overnight with MS-grade trypsin, and the resulting peptide fragments were eluted in 60% acetonitrile:1% trifluoroacetic acid (TFA). The peptide solution was then dried by vacuum centrifugation and resuspended in 1% TFA. The peptides were desalted and concentrated using μC18 ZipTips (Millipore, Billerica, MA, USA), spotted in $0.5 \mu\text{l}$ increments on a stainless steel MALDI target and overlaid with α -cyano-4-hydroxycinnamic acid matrix (Dowd et al., 2008). Peptides were analyzed on an Applied Biosystems 4700 Proteomics Analyzer MALDI-TOF-TOF tandem mass spectrometer (Foster City, CA, USA) in reflector positive mode (MS) with subsequent post-source decay (PSD) and collision-induced dissociation (CID) tandem fragmentation (MS/MS) as previously reported (Dowd et al., 2008; Lee et al., 2006). Peak lists from the resulting MS and MS/MS spectra were searched jointly against both the NCBI and SwissProt non-redundant databases using the Mascot search algorithm (Perkins et al., 1999) with mass error tolerances of 50 p.p.m. for MS and 0.3 Da for MS/MS. The MS/MS spectra were also submitted for automated *de novo* peptide sequencing analysis to both GPS Explorer De Novo Explorer (Applied Biosystems) and PEAKS Studio v4.5 software (Bioinformatics Solutions, Toronto, Canada) (Ma et al., 2003), again with mass error tolerances of 50 p.p.m. for MS and 0.3 Da for MS/MS. The resulting *de novo* amino acid sequences for the tryptic peptides were then searched against the NCBI non-redundant database using MSBLASTP (Shevchenko et al., 2001) and the PEAKS proprietary search engine, respectively. This *de novo* sequencing approach has proven useful in identifying peptides from non-model organisms – including sharks – that do not match predicted peptide mass fingerprint peaks from proteins in bioinformatics databases (Dowd et al., 2008; Lee et al., 2006). Consensus protein identifications were determined based on Mascot (both NCBI and SwissProt), MSBLASTP and PEAKS scores. Matches solely from *de novo* sequencing scores were only accepted when more than 1 peptide matched the protein. When possible, matches were confirmed by agreement of molecular mass (M_r) and isoelectric point (pI) between the database match and the protein

spot of interest on 2-D gels. However, because many of the matched proteins were not sequenced in elasmobranchs, this is not always possible due to sequence differences and/or post-translational modifications of proteins.

Pathway analysis

The lists of changing proteins were analyzed separately for rectal gland and gill using Ingenuity Pathways Analysis (IPA) software (Ingenuity Systems[®], www.ingenuity.com). Identifiers for the mouse or human homologs of the identified proteins were uploaded into IPA, and Gene Ontology (GO) annotations for molecular functions were generated from the manually curated Ingenuity knowledge base. IPA Canonical Pathways Analysis identified the cellular pathways that were significantly represented in the dataset based on a right-tailed Fisher's exact test. The protein identifiers were then overlaid onto a global molecular interaction network developed from the primary literature and contained in the Ingenuity knowledge base. Networks containing the salinity-regulated genes were then algorithmically generated based on their connectivity, with each network assigned a statistical likelihood score (Calvano et al., 2005).

Biochemical assays

Na⁺/K⁺-ATPase activity

The activity of Na⁺/K⁺-ATPase in gill, rectal gland and kidney at 25°C was determined following the method of McCormick (McCormick, 1993), as previously applied to elasmobranchs (Piermarini and Evans, 2000).

Caspase 3/7 activity

Apoptosis-related pathways might be influenced by salinity change in leopard shark tissues, as they are in teleost gill (Kammerer and Kültz, 2009). Thus, we measured the activity of caspases 3 and 7, two proteases that are early effectors of apoptosis, using a luminescent assay (Caspase Glo[™] 3/7 assay kit, Promega, Madison, WI, USA) modified for whole-tissue homogenates (Kammerer and Kültz, 2009). Tissues were homogenized in a lysis buffer (10 mmol l⁻¹ Tris-HCl pH 7.5, 100 mmol l⁻¹ NaCl, 0.1 mmol l⁻¹ EDTA, 0.2% Triton-X100), and caspase activity was normalized to total protein, as determined by a bicinchoninic acid (BCA) assay (Pierce).

Chymotrypsin-like proteasome activity

We measured chymotrypsin-like proteasome activity in gill using a luminescent assay (Proteasome-Glo[™] Chymotrypsin-Like Cell-Based Assay, Promega). Tissues for this assay were homogenized in a hypotonic buffer (10 mmol l⁻¹ Tris-HCl pH 7.5, 5 mmol l⁻¹ MgCl₂, 0.5 mmol l⁻¹ DTT, 5 mmol l⁻¹ ATP) per the manufacturer's recommendation. Proteasome activity was normalized to total protein based on a BCA assay.

Behavioral sampling

To quantify behavioral responses to salinity change in the laboratory, we conducted two types of behavioral sampling. During experiments 1 and 2, we used repeated, 7-minute focal animal sampling intervals (Altmann, 1974). Minutes 1 and 7 were devoted to counting tail-beat frequency, a proxy for swimming speed (Lowe, 1996). Minutes 2–6 were divided into 20-second intervals, and the behavior of the shark in that interval (swimming or resting) was recorded. In experiment 3, we also used a point-sampling approach in which the behavior of each shark (swimming or resting) was recorded every 4–6 h throughout the experiment. Data collected using both of these sampling techniques were analyzed as the proportion of time spent in each behavioral state. In experiment 2 we also counted the number of sharks swimming 3–4 times per day. In all experiments, individuals were distinguished using the unique spot patterns on the dorsal side of the head. For the short-term experiments 1 and 3, the data were collected as salinity was changing.

Statistical analyses

In most cases, treatment groups were compared using one- or two-way analysis of variance (ANOVA) with salinity and/or time as factors as appropriate, and *post hoc* multiple comparisons were carried out using Tukey's Honestly Significant Difference test. Behavioral activity data based on proportions were first arcsine square root transformed. For plasma constituents, we analyzed all data from experiments 1 and 2 together using a mixed-effect model with salinity and time as factors in SAS 9.1.3 (SAS Institute, Cary, NC, USA); we included shark ID in the model to account for the repeated sampling structure in experiment 1. The relationships of liver mass and rectal gland mass with salinity were assessed using analysis of covariance (ANCOVA) with body mass as the covariate. Significance level in all cases was set at $\alpha=0.05$. Normalized protein expression levels of the experimental 2-D gels in the 50% and 75% SW treatments were compared with control 100% SW gels using a *t*-test in Delta 2D software (Dowd et al., 2008). All other statistical analyses were performed in Statistica[®] 6.1 (StatSoft, Tulsa, OK, USA).

RESULTS

Hematological, plasma and tissue analyses

Hematology

There were no differences in HCT among the salinity treatments (Table 1); the two-way ANOVA indicated an effect of time ($P=0.044$) but no effect of salinity ($P=0.152$) or interaction ($P=0.190$). The data from 48 h also indicated no effect of salinity on RBC count ($P=0.627$) or MCV ($P=0.175$) (Table 1).

Plasma constituents

Leopard shark plasma remained iso- or hyperosmotic to the SW medium in all conditions, but plasma osmolality decreased with

Table 1. Hematological variables [hematocrit (HCT, %), mean corpuscular volume (MCV, μm^3), and red blood cell count (RBC, cells mm^{-3})] for leopard sharks exposed to 50–60%, 75–80% or 100% seawater (SW) for 24 h, 48 h and 3 weeks

| Time | | 50–60% SW | N | 75–80% SW | N | 100% SW | N |
|---------|-----|-------------------------|---|-------------------------|---|-------------------------|---|
| 24 h | HCT | 19.3±0.7 ^{a,b} | 6 | 16.6±1.5 ^{a,b} | 6 | 22.7±2.3 ^a | 5 |
| 48 h | HCT | 16.9±1.1 ^{a,b} | 4 | 16.6±0.5 ^{a,b} | 3 | 15.7±1.8 ^b | 4 |
| | MCV | 0.00043±0.00004 | | 0.00044±0.00001 | | 0.00032±0.00003 | |
| | RBC | 408,000±43,000 | | 371,000±31,000 | | 487,000±119,000 | |
| 3 weeks | HCT | 20.2±0.8 ^{a,b} | 3 | 17.0±1.3 ^{a,b} | 3 | 19.0±0.5 ^{a,b} | 3 |

Values are means ± s.e.m. Different lowercase superscripts for HCT indicate statistically different groups, as determined by a two-way ANOVA with time and salinity as factors. There were no differences in MCV or RBC among treatments at 48 h.

salinity to different degrees in the 60% and 80% SW treatments and continued dropping over the 3 weeks ($P_{\text{sal}} < 0.001$, $P_{\text{time}} < 0.001$, $P_{\text{sal} \times \text{time}} < 0.001$) (Fig. 2A–C). The osmotic gradient between the shark and the water was greatest in the 60% treatment at 24 h, while the gradient at 3 weeks was similar in magnitude to that at time 0 h (Fig. 2A). Urea ($P_{\text{sal}} < 0.001$, $P_{\text{time}} < 0.001$, $P_{\text{sal} \times \text{time}} = 0.065$) decreased slightly with decreasing salinity in the 60% SW treatment over 48 h, and subsequently exhibited a dramatic drop at 3 weeks (Fig. 2D). Similarly, urea fluctuated around control

levels up to 48 h in the 80% SW treatment, but it also declined at 3 weeks (Fig. 2E). Leopard sharks maintained their plasma hypoionic to the SW medium. Plasma sodium dropped with decreasing salinity to different degrees in the 60% and 80% SW treatments (Fig. 2G–I) but it stabilized by 48 h in each treatment ($P_{\text{sal}} < 0.001$, $P_{\text{time}} < 0.001$, $P_{\text{sal} \times \text{time}} < 0.001$). Notably, in the 60% SW treatment at 24 h plasma sodium is almost equal to that of the water but the sharks re-established a (smaller) hypoionic gradient by 48 h. Chloride decreased with decreasing salinity in the 60% SW

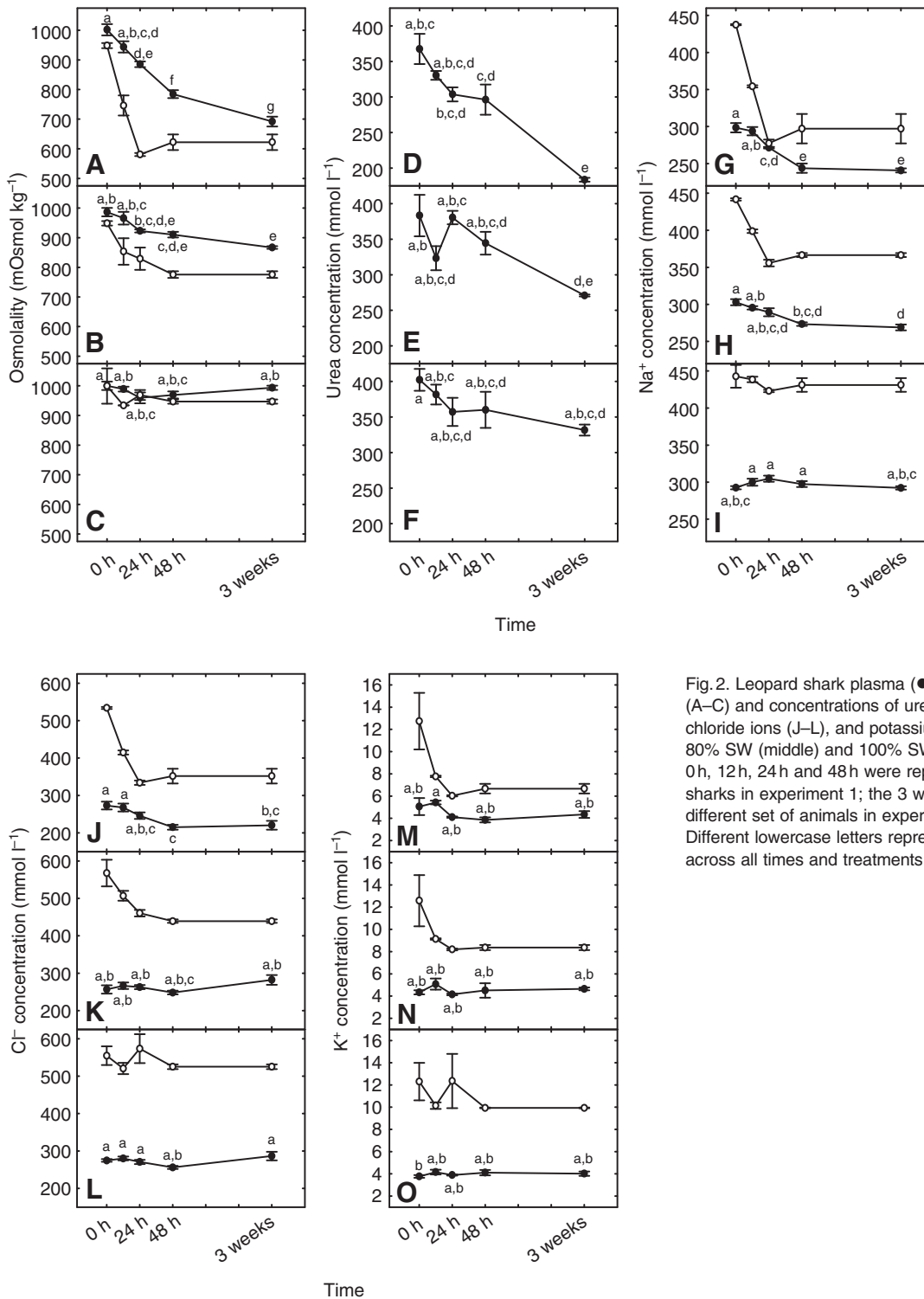


Fig. 2. Leopard shark plasma (●) and seawater (SW) (○) osmolality (A–C) and concentrations of urea (D–F), sodium ions (G–I), chloride ions (J–L), and potassium ions (M–O) in 60% SW (top), 80% SW (middle) and 100% SW (bottom) treatments. Time points 0 h, 12 h, 24 h and 48 h were repeated samples from cannulated sharks in experiment 1; the 3 week samples were obtained from a different set of animals in experiment 2 by caudal puncture. Different lowercase letters represent statistically different groups across all times and treatments for that variable.

treatment but not in the 80% SW treatment ($P_{\text{sal}} < 0.001$, $P_{\text{time}} < 0.001$, $P_{\text{sal} \times \text{time}} = 0.008$) (Fig. 2J–L). However, for unknown reasons the 0h mean chloride concentration for 80% SW was significantly lower ($257 \pm 11 \text{ mmol l}^{-1}$) than for the 60% and 100% SW treatments (273 ± 10 and $274 \pm 4 \text{ mmol l}^{-1}$, respectively). Plasma potassium concentrations were more tightly regulated across salinity treatments ($P_{\text{sal}} = 0.052$), although there was a small effect of time ($P_{\text{time}} = 0.0191$, $P_{\text{sal} \times \text{time}} = 0.147$) (Fig. 2M–O). Plasma protein content decreased with salinity at both the 48 h and 3 week time points ($P_{\text{sal}} < 0.001$, $P_{\text{time}} = 0.811$, $P_{\text{sal} \times \text{time}} = 0.357$) (Fig. 3A), suggesting hemodilution.

Tissue analyses

The 50–60% SW and 75–80% SW treatments gained muscle moisture, and it stabilized by 48 h ($P_{\text{sal}} < 0.001$, $P_{\text{time}} = 0.003$, $P_{\text{sal} \times \text{time}} = 0.202$) (Fig. 3B). Animals also gained weight in the 50–60% SW ($9.0 \pm 1.2\%$ body mass) and 75–80% SW ($1.9 \pm 0.8\%$ body mass) treatments in the 48 h experiment despite not feeding, further supporting water influx. There was no effect of salinity on liver mass (ANCOVA, $P = 0.793$). Meanwhile, rectal gland mass tended to decrease slightly in sharks exposed to lower salinities for both the 48 h and 3 week treatments (ANCOVA, $P < 0.001$).

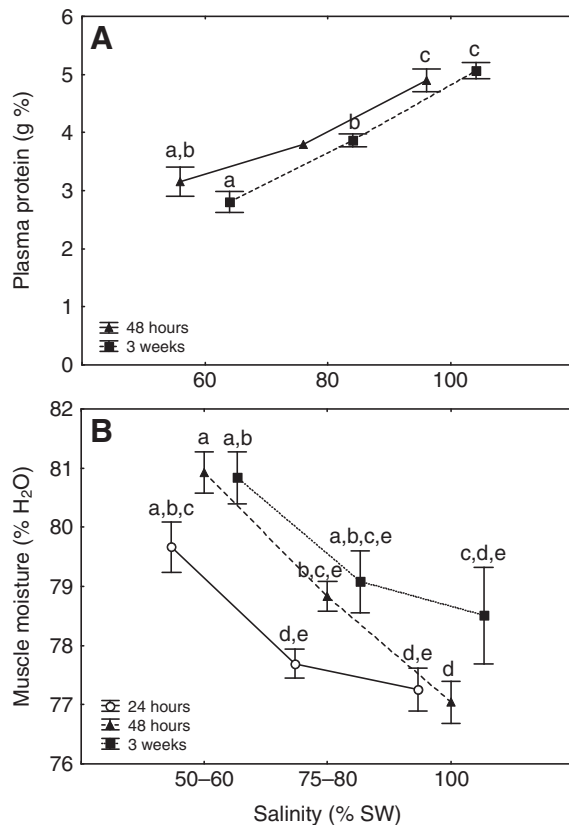


Fig. 3. Plasma protein concentration (A) and muscle moisture content (B) for leopard sharks exposed to salinity changes in experiments 1 (48 h), 2 (3 weeks) and 3 (24 h). Different lowercase letters represent statistically different groups, as determined by two-way ANOVA with time and salinity as factors. Due to technical failures only one data point was obtained at 80% SW for 48 h; this time point was excluded from the statistical analysis.

Proteomics

Rectal gland

The master gel image for rectal gland contained 588 protein spots that were quantified (Fig. 4). The abundance of 11 spots changed significantly in the 75% SW treatment relative to 100% SW controls (7 decreased, 4 increased), and 22 spots changed abundance significantly in the 50% SW treatment relative to 100% SW controls (16 decreased, 6 increased) (Table 2). Of the 28 total protein spots regulated by salinity change, 20 (71%) were identified using MS combined with bioinformatics searches (Table 2). Other protein spots yielded high quality mass spectra that did not produce matches in any of the database searches.

Based on GO annotations and a manual review of the literature, we categorized the identified proteins according to their likely functions (Table 2). Several proteins related to energy (i.e. ATP) production (glycolysis, TCA cycle, malate aspartate shuttle) decreased in abundance. Seven spots were identified as the mitochondrial ATP synthase alpha subunit, two of which increased in abundance in 50% SW while four decreased (Table 2). This phenomenon is common in 2-D gel studies (e.g. Dowd et al., 2008), and it suggests post-translational modifications such as (de)phosphorylation of the corresponding proteins. Overall, this protein expression pattern suggests a decrease in oxidative phosphorylation at 50% salinity in rectal gland, consistent with other aspects of energy metabolism. There were also consistent decreases in heterogeneous nuclear ribonucleoproteins and PRP4 pre-mRNA processing factor, all related to transcription and mRNA processing. Three keratins involved in the stability of the cytoskeleton also decreased. By contrast, creatine kinase and methylmalonate-semialdehyde dehydrogenase both increased in 50% SW. Five protein spots were consistently up- or downregulated in both treatments (Table 2); two of them were identified as H⁺-transporting ATP synthase alpha subunit (increased both treatments) and

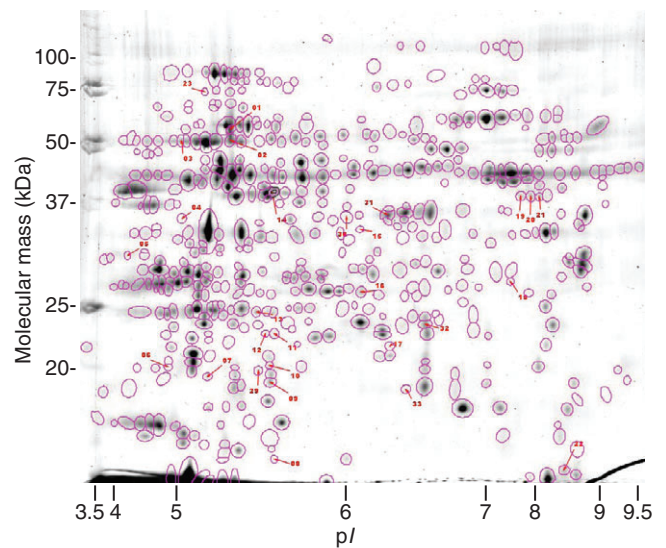


Fig. 4. Master 2-D gel for leopard shark rectal gland at 24 h, formed by warping and fusing 16 individual gel images together in Delta 2D software. Protein mixtures were separated by isoelectric point (pI) in the horizontal dimension and molecular mass in the vertical dimension. Outlines represent the 588 protein spots analyzed across the three salinity treatments, and red labels indicate spots that were significantly up- or downregulated in 50% and/or 75% seawater (SW) relative to 100% SW controls.

Table 2. Expression ratios [relative to control 100% seawater (SW)] and mass spectrometry (MS) identification scores for leopard shark rectal gland proteins regulated by salinity change

| | Expression ratios | | | Protein identification (abbreviation) | Accession | | Mascot | | MSBLASTP | | PEAKS | | M _r theor (kDa) | pI theor (pH) | M _r gel (kDa) | pI gel (pH) | | |
|-------------------------------------|-------------------|-------------|--------------|---------------------------------------|--------------|--------------|--------|-----|----------|---------|---------|--------|----------------------------|---------------|--------------------------|-------------|------|------|
| | Spot | 50% P | 75% P | | No. | PSD | Cov. | CID | Cov. | PSD | PSD | CID | | | | | CID | |
| (i) Glycolysis | 31 | 1.03 | 0.942 | 0.45 | 0.028 | gli30288616 | 125 | 47 | - | - | - | - | 6.3 | 31.9 | 6 | 32.3 | | |
| | | | | | | | | | | | | | | | | | | |
| | 16 | 0.47 | 0.023 | 0.54 | 0.078 | gli28630226 | 150 | 20 | - | 109 (2) | - | - | 7.8 | 34.1 | 5.9 | 26.2 | | |
| (ii) TCA cycle | 13 | 0.3 | 0.046 | 0.29 | 0.063 | gli68161102 | - | - | 125 | 17 | - | - | 6.5 | 26.1 | 5.4 | 24.6 | | |
| | | | | | | | | | | | | | | | | | | |
| (iii) Malate aspartate shuttle | 15 | 0.48 | 0.019 | 0.94 | 0.747 | gli29242787 | 111 | 23 | 88 | 12 | 182 (3) | 91 (3) | 91 (2) | 6.9 | 36.3 | 5.9 | 32.5 | |
| (iv) Phosphocreatine circuit | 14 | 2.31 | 0.027 | 2 | 0.164 | gli28630226 | 206 | 47 | 157 | 57 | - | 99 (6) | 42 (3) | 7.8 | 34.1 | 5.5 | 38.1 | |
| (v) Oxidative phosphorylation | 2 | 2.09 | 0.049 | 1.24 | 0.522 | gli28630334 | 156 | 22 | 210 | 35 | - | 90 (3) | 96 (3) | 9.4 | 39.5 | 5.2 | 50 | |
| | 3 | 2.09 | 0.037 | 2.2 | 0.043 | gli148223147 | 379 | 34 | 420 | 32 | 190 (4) | 99 (5) | 99 (6) | 9.1 | 10 | 4.8 | 49.5 | |
| | 12 | 0.27 | 0.029 | 0.47 | 0.124 | gli28630332 | 198 | 29 | 99 | 24 | - | 94 (4) | 77 (4) | 9.5 | 39.6 | 5.5 | 23.1 | |
| | 11 | 0.3 | 0.041 | 0.39 | 0.102 | gli28630332 | 254 | 26 | 183 | 25 | 247 (4) | 99 (4) | 95 (4) | 9.5 | 39.6 | 5.5 | 23 | |
| | 17 | 0.35 | 0.009 | 0.67 | 0.265 | gli118562406 | 160 | 30 | 153 | 32 | 98 (2) | 93 (3) | 98 (3) | 5.3 | 16.9 | 6 | 22.3 | |
| | 22 | 0.25 | 0.028 | 0.29 | 0.052 | gli47207317 | 378 | 22 | 206 | 22 | 113 (2) | 99 (7) | 94 (4) | 9.2 | 59.8 | 8.2 | 16.7 | |
| | 23 | 0.84 | 0.656 | 0.39 | 0.009 | gli28630334 | 81 | 22 | 138 | 25 | - | 53 (3) | - | 9.3 | 39.4 | 5 | 69.1 | |
| (vi) Amino acid metabolism | 1 | 2.44 | 0.031 | 1.19 | 0.584 | gli116487892 | 73 | 10 | - | - | - | 69 (2) | 74 (2) | 8.5 | 36.3 | 5.2 | 53.4 | |
| (vii) mRNA processing and transport | 7 | 0.25 | 0.016 | 0.22 | 0.018 | gli1350822 | 69 | 18 | - | - | 107 (2) | - | - | 9.2 | 34.4 | 5 | 20.6 | |
| | 10 | 0.45 | 0.027 | 0.59 | 0.152 | gli58801248 | 43 | 30 | 37 | 16 | - | 72 (3) | - | 7.8 | 22.1 | 5.5 | 21.2 | |
| | 29 | 0.44 | 0.096 | 0.42 | 0.029 | gli109132046 | 134 | 23 | 136 | 23 | - | 78 (2) | 82 (3) | 9 | 27.4 | 5.4 | 18.6 | |
| (viii) Cytoskeleton | 18 | 0.48 | 0.011 | 0.65 | 0.094 | gli23831382 | 118 | 16 | 182 | 23 | 151 (3) | - | - | 10 | 11.7 | 7 | 27 | |
| | 19 | 0.37 | 0.007 | 0.8 | 0.641 | gli2909610 | 101 | 23 | - | - | - | - | - | 6.1 | 50.8 | 7.2 | 37.4 | |
| | 20 | 0.32 | 0.01 | 0.63 | 0.297 | gli2909610 | 76 | 14 | - | - | 243 (5) | 96 (4) | - | 6.1 | 50.8 | 7.5 | 37.5 | |
| | 21 | 0.44 | 0.01 | 0.64 | 0.265 | gli82190152 | 215 | 44 | - | - | 167 (3) | 99 (7) | - | 5.2 | 46.8 | 7.7 | 37.5 | |
| (ix) Unidentified | 4 | 2.84 | 0.02 | 2.62 | 0.017 | - | - | - | - | - | - | - | - | - | - | - | 4.8 | 33.9 |
| | 5 | 2.26 | 0.046 | 3.89 | 0.027 | - | - | - | - | - | - | - | - | - | - | - | 3.8 | 29.6 |
| | 6 | 0.48 | 0.01 | 0.7 | 0.107 | - | - | - | - | - | - | - | - | - | - | - | 4.6 | 21.1 |
| | 8 | 0.27 | 0.029 | 0.76 | 0.562 | - | - | - | - | - | - | - | - | - | - | - | 5.5 | 17 |
| | 9 | 0.47 | 0.013 | 0.55 | 0.039 | - | - | - | - | - | - | - | - | - | - | - | 5.5 | 20.3 |
| | 30 | 0.5 | 0.133 | 0.31 | 0.044 | - | - | - | - | - | - | - | - | - | - | - | 5.9 | 31.8 |
| | 32 | 1.65 | 0.152 | 4.08 | 0.024 | - | - | - | - | - | - | - | - | - | - | - | 6.2 | 21.4 |
| | 33 | 0.68 | 0.137 | 0.39 | 0.023 | - | - | - | - | - | - | - | - | - | - | - | 6.1 | 17.7 |

Proteins were grouped by putative function based on Gene Ontology annotations and a manual review of the literature. Values in bold font met both the statistical ($P < 0.05$) and expression ratio (< 0.5 or > 2.0) criteria for MS analysis in that treatment. Data from both post-source decay (PSD) and collision-induced dissociation (CID) MS/MS modes were searched against the SwissProt and NCBI non-redundant sequence databases. Sequence coverage for peptide mass fingerprint spectra (Cov.; % of overall sequence) are shown for Mascot matches. The numbers of *de novo* sequenced peptides from MS/MS spectra that matched the protein in MSBLASTP and PEAKS searches are shown in parentheses after the scores. Isoelectric point (pI) and molecular mass (M_r) are presented for both the top database hit (theoretical, theor.) and from the leopard shark gels (gel).

heterogeneous nuclear ribonucleoprotein A1 (decreased both treatments).

We focused on the pathway analysis results for the 50% SW treatment, because only three proteins mapped to a single network in the 75% SW treatment. This network was associated with functions in *DNA Replication, Recombination, and Repair; Post-Translational Modification; and Cancer* ($P=10^{-8}$). The 20 identified proteins in the 50% SW list matched to 12 unique protein identifiers in IPA. The top GO functions associated with these proteins were (1) cellular assembly and organization (KRT8 and KRT18: stabilization, organization and quantity of keratin filaments, $P=5.6\times 10^{-7}$; CKM: aggregation of cellular membrane, $P=0.002$), (2) cell-to-cell signaling and interaction (KRT8 and KRT18: activation of fibroblast cell lines, $P=1.6\times 10^{-5}$), (3) amino acid metabolism (ALDH6A1: catabolism of β -alanine, $P=7.9\times 10^{-4}$), (4) carbohydrate metabolism (CKM: quantity and consumption of glycogen, $P=7.9\times 10^{-4}$; PGAM2: flux of glucose, $P=5.5\times 10^{-3}$), (5) cellular compromise (KRT18: collapse of keratin filaments, $P=7.9\times 10^{-4}$). The top canonical pathways associated with the dataset were inositol metabolism (ALDH6A1, $P=0.01$), glyoxylate and dicarboxylate metabolism (MDH1, $P=0.01$), citrate cycle (MDH1, IDH2, $P=0.02$), urea cycle and metabolism of amino groups (CKM, $P=0.02$), and β -alanine metabolism (ALDH6A1, $P=0.04$). The protein list mapped to one network with functions associated with *Antigen Presentation, Antimicrobial Response, and Cell-mediated Immune Response* ($P=10^{-30}$) (see Fig. S1 in supplementary material).

Gill

The master gel image for gill contained 1037 protein spots that were quantified. Abundances of 70 spots changed significantly in the 50% SW treatment (45 decreased, 25 increased) relative to 100% SW controls (Table 3). Of these 70 spots, 26 (37%) were identified using MS combined with bioinformatics searches (Table 3).

The gill proteins were categorized in the same manner as for rectal gland (Table 2). As for rectal gland, proteins involved in energy production (ALDOA in glycolysis), transcription/translation (UBTF, TOP1, EEF2) and the cytoskeleton (EZR, PLS3, ACTB) decreased with decreasing salinity. There were fewer changes associated with energy production in gill than in rectal gland. Notably, several components of the 26S proteasome (PSMD12, PSMC2, PSMA2) were identified in one or more spots that changed in abundance in gill, including pairs of protein spots with opposite changes in expression that suggest post-translational modifications of proteasome constituents [e.g. (de)phosphorylation] with salinity change.

The 26 identified gill proteins regulated by salinity change matched to 19 unique identifiers in IPA. The top GO functions associated with these proteins were (1) amino acid metabolism (DDAH1, OAT, PEPD: arginine and ornithine metabolism, 5.3×10^{-4} ; PMM2: glycosylation of amino acids, $P=0.05$), (2) small molecule biochemistry (PMM2: biosynthesis of GDP-D-mannose, $P=0.001$; CPOX: biosynthesis of heme, $P=0.01$; DDAH1: biosynthesis of nitric oxide, $P=0.04$; PPA1: formation of ADP-D-ribose, $P=0.001$), (3) DNA replication, recombination and repair (TOP1, UBTF: conformational modification of DNA, $P=0.001$), (4) carbohydrate metabolism (PMM2: biosynthesis of GDP-D-mannose, $P=0.001$; PPA1: formation of ADP-D-ribose, $P=0.001$; GAPDH: quantity of UDP-N-acetylglucosamine, $P=0.006$), and (5) cell cycle (TOP1: organization of nucleoli, $P=0.003$; GAPDH: length of telomeres, $P=0.04$). The top canonical pathways associated with the dataset were fructose and

mannose metabolism (PMM2, ALDOA, $P=0.003$), glycolysis/gluconeogenesis (ALDOA, GAPDH, $P=0.009$), protein ubiquitination pathway (PSMD12, PSMC2, PSMA2, $P=0.02$) and inositol metabolism (ALDOA, $P=0.02$). The protein list mapped to three IPA networks with functions associated with (i) *DNA Replication, Recombination, and Repair, Cancer, Cell Death* ($P=10^{-45}$), (ii) *Cell Cycle, Cell Death, Cell-mediated Immune Response* ($P=0.01$), and (iii) *Carbohydrate Metabolism, Nucleic Acid Metabolism, Small Molecule Biochemistry* ($P=0.01$) (see Fig. S2 in supplementary material).

Biochemical assays

Na⁺/K⁺-ATPase activity

The activity of Na⁺/K⁺-ATPase exhibited different patterns for the three tissues assayed. Gill demonstrated consistently low activity across all treatments and times ($P_{\text{sal}}=0.971$, $P_{\text{time}}=0.864$) (Table 4). In the rectal gland, Na⁺/K⁺-ATPase activity in the 50% SW treatment tended to decrease relative to the other treatments at 24 h ($P_{\text{sal}}=0.011$) (Table 4). Unfortunately, we did not have sufficient tissue to assess changes in rectal gland activity at 3 weeks. Kidney Na⁺/K⁺-ATPase activity increased in the lower salinity treatments, doubling in 50–60% SW at 3 weeks ($P_{\text{sal}}<0.001$, $P_{\text{time}}<0.001$) (Table 4).

Caspase activity

There were no significant effects of salinity on normalized caspase 3/7 activity in either gill ($P=0.706$) or rectal gland ($P=0.197$) at 24 h (Table 5). Overall, relative caspase activity was higher in gill, which may reflect higher constitutive levels of cell turnover in this tissue than in rectal gland.

Chymotrypsin-like proteasome activity

There was no significant effect of salinity ($P=0.752$) or time ($P=0.989$) on gill chymotrypsin-like proteasome activity (Table 5).

Behavioral sampling

In the short-term experiments, there was a significant effect of salinity on swimming activity at 24 h ($P=0.046$) (Fig. 5A), with the 50–60% SW group spending a greater proportion of time swimming. We found similar, but statistically insignificant, trends for swimming activity ($P=0.285$) and tail-beat frequency ($P=0.171$) for 48 h. The number of behavioral changes (blocks of time in which both rest and swim occurred) did decrease with decreasing salinity in the 48 h experiment ($P=0.016$), suggesting that the sharks were swimming more consistently at lower salinities. In the 3 week treatment the pattern of activity was reversed, with fewer sharks active in the 60% SW group compared with the other treatments based on the point sampling data (Kruskal–Wallis ANOVA: $H_{2,47}=22.00$, $P<0.001$). Tail-beat frequency ($P=0.291$) and swimming activity ($P=0.314$) for 3 weeks exhibited similar, although insignificant, trends (Fig. 5B); discriminatory power at 3 weeks was limited by relatively small sample sizes.

DISCUSSION

Salinity change has profound effects on leopard sharks at multiple levels of organization, from proteins to behavior. The integration of proteomics with traditional physiological measurements and behavioral data for a species with unremarkable salinity tolerance allows us to describe some of the potential trade-offs inherent in the use of estuaries by partially euryhaline elasmobranchs and suggests novel paths for future research.

Table 3. Expression ratios [relative to control 100% seawater (SW)] and mass spectrometry identification scores for leopard shark gill proteins regulated by salinity change

| Spot | Expression ratio | P | Protein identification (abbreviation) | Accession No. | | Mascot | | MSBLASTP | | PEAKS | | M _r theor (kDa) | pI theor (pH) | M _r gel (kDa) | pI gel (pH) | M _r gel (kDa) |
|--|------------------|--------|--|---------------|------|--------|-----|----------|---------|---------|---------|----------------------------|---------------|--------------------------|-------------|--------------------------|
| | | | | PSD | Cov. | Cov. | CID | PSD | CID | PSD | CID | | | | | |
| (i) Glycolysis | | | | | | | | | | | | | | | | |
| 57 | 0.34 | 0.004 | Fructose-bisphosphate aldolase A (<i>Cephaloscyllium umbratile</i>) (ALDOA) | gi46849443 | 83 | 9 | 110 | 4 | - | - | - | 8.2 | 36.2 | 5.9 | 19.7 | |
| 27 | 3.77 | 0.007 | Glyceraldehyde-3-phosphate dehydrogenase (<i>Triakis scyllium</i>) (GAPDH) | gi30268616 | - | - | 112 | 19 | - | - | - | 6.3 | 31.9 | 6.1 | 32.6 | |
| 28 | 0.27 | 0.002 | Glyceraldehyde-3-phosphate dehydrogenase (<i>Triakis scyllium</i>) (GAPDH) | gi30268616 | - | - | 87 | 31 | - | - | - | 6.3 | 31.9 | 6 | 31.8 | |
| (ii) Metabolism of phosphate groups | | | | | | | | | | | | | | | | |
| 33 | 0.19 | 0.001 | Pyrophosphatase, inorganic (<i>Danio rerio</i>) (PPA1) | gi47208357 | - | - | 172 | 24 | - | 11 (2) | 99 (2) | 5 | 33.3 | 6 | 28.8 | |
| 34 | 2.55 | 0.007 | Pyrophosphatase, inorganic (<i>Danio rerio</i>) (PPA1) | gi47208357 | - | - | - | - | - | 70 (2) | - | 5 | 33.3 | 5.9 | 28.8 | |
| (iii) Transcription and translation | | | | | | | | | | | | | | | | |
| 66 | 0.46 | 0.005 | Upstream binding transcription factor, RNA polymerase I (<i>Mus musculus</i>) (UBTF) | gi123241494 | 86 | 29 | - | - | - | 63 (2) | - | 7.7 | 18.4 | 4.8 | 22 | |
| 14 | 0.39 | 0.042 | DNA topoisomerase I (<i>Chlorocebus aethiops</i>) (TOP1) | gi38503303 | 127 | 24 | 118 | 26 | - | - | - | 9.3 | 91.4 | 6.1 | 58.1 | |
| 10 | 0.49 | 0.031 | Eukaryotic translation elongation factor 2, like (<i>Danio rerio</i>) (EEF2) | gi41386743 | 118 | 15 | - | - | 108 (2) | 88 (5) | - | 6.3 | 96.5 | 4.9 | 77 | |
| (iv) Vaults | | | | | | | | | | | | | | | | |
| 4 | 0.32 | <0.001 | Major vault protein (Fragment) (<i>Ictalurus punctatus</i>) (MVP) | gi33860179 | 65 | 15 | - | - | - | 68 (2) | - | 5.37 | 98 | 6.7 | 79.1 | |
| (v) Cytoskeleton | | | | | | | | | | | | | | | | |
| 12 | 0.47 | 0.026 | Ezrin (<i>Homo sapiens</i>) (EZR) | gi46249758 | 143 | 21 | 101 | 18 | 159 (3) | - | 88 (4) | 6.33 | 68.6 | 5.9 | 60.9 | |
| 15 | 0.29 | 0.008 | Plastin 3 (<i>Homo sapiens</i>) (PLS3) | gi14250317 | 73 | 21 | - | - | - | 92 (2) | - | 6.2 | 46.2 | 6.3 | 52.3 | |
| 45 | 0.48 | 0.004 | Beta actin (cytoplasmic) (<i>Rattus norvegicus</i>) (ACTB) | gi149034975 | 157 | 48 | - | - | 106 (2) | 83 (5) | 43 (2) | 6.1 | 16.7 | 6.3 | 26.7 | |
| (vi) Proteasome | | | | | | | | | | | | | | | | |
| 18 | 0.45 | 0.022 | Proteasome 26S subunit, non-ATPase subunit 12 (<i>Xenopus tropicalis</i>) (PSMD12) | gi2858399 | - | - | - | - | - | 78 (1) | 48 (2) | 5.9 | 51.4 | 6 | 43.2 | |
| 20 | 0.03 | <0.001 | Proteasome (prosome, macropain) 26S subunit, ATPase 2 (<i>Rattus norvegicus</i>) (PSMC2) | gi38181888 | 742 | 69 | 696 | 68 | 71 (2) | 99 (13) | 99 (12) | 5.85 | 49 | 6 | 39 | |
| 21 | 0.13 | 0.007 | Proteasome (prosome, macropain) 26S subunit, ATPase 2 (<i>Pongo abelii</i>) (PSMC2) | gi197098688 | 161 | 47 | 144 | 46 | - | - | - | 5.84 | 46.2 | 6 | 39.3 | |
| 22 | 3.16 | 0.008 | Proteasome (prosome, macropain) 26S subunit, ATPase 2 (<i>Danio rerio</i>) (PSMC2) | gi41055738 | 827 | 64 | 597 | 48 | 111 (2) | 99 (14) | 99 (11) | 5.71 | 49 | 6 | 39.4 | |
| 61 | 0.22 | 0.002 | Proteasome (prosome, macropain) subunit, alpha type, 2 (<i>Danio rerio</i>) (PSMA2) | gi66773056 | 351 | 43 | - | - | 315 (6) | 99 (6) | - | 6 | 25.9 | 5.9 | 24.4 | |
| 62 | 2.12 | 0.004 | Proteasome (prosome, macropain) subunit, alpha type, 2 (<i>Danio rerio</i>) (PSMA2) | gi66773056 | - | - | 156 | 39 | - | - | 92 (5) | 6 | 25.9 | 5.9 | 24.4 | |
| 64 | 0.43 | <0.001 | Novel protein similar to vertebrate proteasome (prosome, macropain) subunit, alpha type 2 (<i>Danio rerio</i>) (PSMA2) | gi94732607 | 251 | 38 | 202 | 38 | - | 93 (4) | 92 (5) | 9.6 | 23.9 | 5.7 | 24.7 | |
| 65 | 2.20 | 0.002 | Novel protein similar to vertebrate proteasome (prosome, macropain) subunit, alpha type 2 (<i>Danio rerio</i>) (PSMA2) | gi94732607 | 217 | 39 | 143 | 38 | - | 98 (5) | 96 (3) | 9.6 | 23.9 | 5.6 | 24.7 | |
| (vii) Amino acid metabolism and urea cycle | | | | | | | | | | | | | | | | |
| 16 | 0.38 | 0.002 | Peptidase D (<i>Rattus norvegicus</i>) (PEPD) | gi57528238 | - | - | - | - | - | 47 (2) | 26 (2) | 5.5 | 54.7 | 6.1 | 45.6 | |
| 29 | 2.60 | 0.031 | Dimethylarginine dimethylaminohydrolase 1 (<i>Danio rerio</i>) (DDA1H) | gi148725537 | - | - | - | - | - | 90 (2) | 90 (1) | 5.2 | 31 | 5.7 | 30.8 | |
| 69 | 0.31 | 0.003 | Omitine aminotransferase (<i>Mus musculus</i>) (OAT) | gi83938666 | 69 | 3 | - | - | 340 (6) | 90 (2) | - | 6.1 | 48.4 | 6.1 | 39.3 | |
| (viii) Membrane binding | | | | | | | | | | | | | | | | |
| 42 | 0.17 | 0.001 | Annexin A4 (<i>Rattus norvegicus</i>) (ANXA4) | gi149036643 | 160 | 24 | 76 | 48 | 111 (2) | 97 (2) | 85 (2) | 5.3 | 33.6 | 6 | 27.6 | |
| (ix) Glycoprotein biosynthesis | | | | | | | | | | | | | | | | |
| 44 | 0.24 | 0.003 | Phosphomannomutase 2 (<i>Danio rerio</i>) (PMM2) | gi41056095 | 72 | 6 | - | - | 66 (1) | 75 (2) | - | 5.6 | 28.7 | 6.1 | 26.4 | |
| (x) Heme biosynthesis | | | | | | | | | | | | | | | | |
| 55 | 2.42 | 0.002 | Coproporphyrinogen oxidase (<i>Tetraodon nigroviridis</i>) (CPOX) | gi47225709 | 82 | 23 | - | - | - | 41 (2) | - | 7.8 | 50.9 | 6.1 | 20.3 | |

Proteins were grouped by putative function based on Gene Ontology annotations and manual review of the literature. Protein spots that were not identified are not included. Data in remaining columns as in Table 2.

Table 4. Activities of Na⁺/K⁺-ATPase (μmol ADP h⁻¹ mg⁻¹ protein) in leopard shark rectal gland, gill and kidney homogenates after salinity change in experiment 3 (24 h) and experiment 2 (3 weeks)

| Tissue | Time | 50–60% SW | N | 75–80% SW | N | 100% SW | N |
|--------------|------|--------------------------|---|--------------------------|---|---------------------------|---|
| Rectal gland | 24 h | 49.12±2.01 ^a | 6 | 63.98±3.83 ^b | 6 | 55.92±2.94 ^{a,b} | 5 |
| Gill | 24 h | 0.30±0.14 | 6 | 0.30±0.09 | 6 | 0.27±0.06 | 5 |
| | 3 wk | 0.29±0.08 | 3 | 0.27±0.13 | 3 | 0.26±0.04 | 3 |
| Kidney | 24 h | 1.09±0.11 ^{b,c} | 6 | 0.91±0.15 ^{b,c} | 6 | 0.70±0.03 ^c | 5 |
| | 3 wk | 2.07±0.04 ^a | 3 | 1.36±0.13 ^b | 3 | 1.09±0.16 ^{b,c} | 3 |

Values are means ± s.e.m. Lowercase superscripts indicate statistically different groups within each tissue, as determined by two-way ANOVA with time and salinity as factors. SW, seawater.

Table 5. Caspase 3/7 activity and chymotrypsin-like proteasome activity in leopard shark rectal gland and gill homogenates after salinity change in experiment 3 (24 h) and experiment 2 (3 weeks)

| Tissue | Activity | 50–60% SW | N | 75–80% SW | N | 100% SW | N |
|--------------|--------------------|----------------|---|----------------|---|----------------|---|
| Rectal gland | Caspase 3/7 24 h | 1571±220 | 6 | 2611±633 | 6 | 2675±362 | 4 |
| Gill | Caspase 3/7 24 h | 17,772±1795 | 6 | 13,968±3911 | 6 | 16,095±3863 | 5 |
| | Proteasome 24 h | 396,133±26,329 | 6 | 344,223±45,015 | 6 | 381,978±64,287 | 5 |
| | Proteasome 3 weeks | 386,277±86,447 | 3 | 431,432±26,730 | 3 | 301,548±71,377 | 3 |

Activities were determined by luminescent assays [relative light units (RLU)] and were normalized to total protein. Values are means ± s.e.m. (RLU mg⁻¹ protein). There were no significant differences with salinity. SW, seawater.

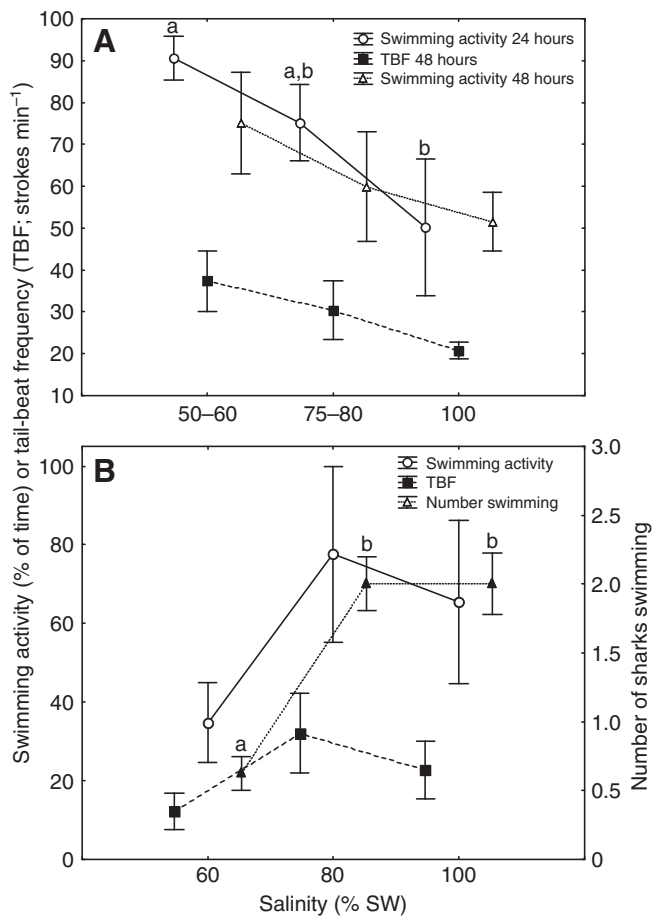


Fig. 5. Short-term (A, 24 h and 48 h) and long-term (B, 3 weeks) behavioral responses of leopard sharks to salinity change, as determined by focal animal sampling and point sampling techniques. Different lowercase letters represent significant effects of salinity on two of the behavioral measurements.

Leopard sharks ionoregulate while osmoconforming, with a lag

When faced with decreases in salinity, partially euryhaline elasmobranchs such as the leopard shark eventually re-establish their slightly hyperosmotic status by selectively losing urea (and possibly other plasma constituents not measured in the present study) while maintaining ion concentrations. Notably, the adjustments in plasma osmolality, urea and ion concentrations in leopard sharks lagged behind the changes in the medium, similar to patterns in other elasmobranchs (Cooper and Morris, 1998; Pillans et al., 2005). Some of our physiological measurements indicate active regulation in response to salinity change, while others are more indicative of passive movements of water and plasma constituents. The hematological results revealed no effect of salinity on HCT or RBC characteristics, as found in other elasmobranch studies (e.g. Janech et al., 2006; Sulikowski et al., 2003). Similarly, plasma concentrations of sodium, chloride and potassium ions either remained unchanged or stabilized at new, lower levels by 48 h that persisted over the 3 weeks. Interestingly, the fairly rapid decreases in leopard shark rectal gland Na⁺/K⁺-ATPase activity and size within 24 h are analogous to, but less severe than, those observed in rectal glands of elasmobranchs acclimated to FW for longer periods (Piermarini and Evans, 2000; Pillans et al., 2005). These changes are consistent with a reduced physiological capacity for NaCl excretion in dilute seawater, despite the persistent, but reduced, inwardly directed Na⁺ and Cl⁻ gradients in leopard sharks.

Given that leopard sharks are very rarely captured near or below 50% SW, our data are consistent with the hypotheses that partially euryhaline sharks cannot switch from net ion excretion to net ion uptake and also cannot defend large hyperosmotic gradients. These physiological limitations contrast with the abilities of truly euryhaline elasmobranchs in FW (Janech et al., 2006; Pillans and Franklin, 2004; Pillans et al., 2005). It is possible that partially euryhaline elasmobranchs simply cannot regulate the abundances or activities of necessary epithelial transporters when facing dilute salinity. Plasma urea decreased in the long-term in leopard sharks

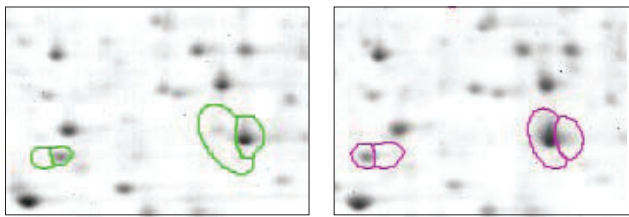


Fig. 6. Close-up of 2-D gel images from leopard shark gill 24 h after change to 100% seawater (SW) (controls, left) and 50% SW (right). Outlines indicate two pairs of protein spots, all four identified as proteasome alpha type 2 (left pair: 61, 62; right pair: 64, 65 in Table 3), that changed isoelectric points between the two treatments.

exposed to 50–60% or 75–80% SW, driving the continued decreases in plasma osmolality at 3 weeks. Given the evidence for decreased urea production in lower salinities for both euryhaline (Anderson et al., 2005) and partially euryhaline elasmobranchs (Steele et al., 2005), differences in the ability to retain urea probably contribute to differences in salinity tolerance between these two groups. Consistent with this idea and with our data, other partially euryhaline species increase urea loss in dilute seawater (Steele et al., 2005).

Elasmobranch epithelial membrane permeabilities to urea are already quite low in SW (Zeidel et al., 2005; Wood et al., 1995) and, at least in gill, are reinforced by active transport of urea back into the plasma (Fines et al., 2001). Interestingly, our proteomics data suggest decreased urea production at low salinity within gill cells themselves. The decrease in OAT (all abbreviations as in Tables 2 and 3) abundance implies reduced conversion of ornithine to glutamate for entry into the urea cycle (Ballantyne, 1997). The increase in DDAH1, which catalyzes the conversion of dimethylarginine to dimethylamine and citrulline, also may reduce the availability of arginine for the urea cycle. Extrahepatic urea cycle activity in elasmobranchs has recently been demonstrated (Steele et al., 2005), and our data suggest that several elasmobranch tissues may adjust urea production according to environmental conditions.

Proteomics reveals coordinated responses to salinity change

Given the changes we found in plasma composition, it follows that leopard shark cells, even those not exposed directly to the environment, would be osmotically challenged by reduced water salinity. For example, decreases in total intracellular urea and TMAO concentrations and/or the ratio of these counteracting osmolytes may have significant effects on shark enzyme structure and function (Hochachka and Somero, 2002; Yancey and Somero, 1978). Our proteomics results and pathway modeling indicated a coordinated, fairly rapid (within 24 h) response of several functional processes to salinity change in leopard shark tissues. Several of the identified proteins (e.g. GAPDH, IDH2, TOP1) are represented in the highly conserved ‘minimal stress proteome’ (Kültz, 2003; Kültz, 2005), although they were largely downregulated here rather than being induced, as would be expected under ‘stressful’ conditions. Similar functions are influenced by decreasing salinity in the leopard shark rectal gland as were regulated in response to salt loading after feeding in the rectal gland of spiny dogfish (*Squalus acanthias*) (Dowd et al., 2008), although largely in the direction of gland inactivation in the current context. Exposure to hyposmotic conditions also influences similar proteins and biological processes to those involved in the hyperosmotic response of a euryhaline teleost (tilapia, *Oreochromis mossambicus*) (Fiol et al., 2006). We also found that

more proteins were regulated in rectal gland by a more extreme physiological disturbance (i.e. more changes in 50% SW than in 75% SW).

Regulation of intracellular osmolytes and energy producing and consuming processes

Gill and rectal gland exhibited several common responses after exposure to 50% SW, including changes in expression of proteins involved in the regulation of intracellular osmolyte pools. Both tissues exhibited changes in the abundance of proteins associated with GO annotations for amino acid metabolism (of which DDAH1 and OAT in gill were discussed above). Several amino acids are important secondary osmolytes in elasmobranch osmoregulation, particularly intracellularly, and some (e.g. β -alanine, proline) have been shown to decrease with decreasing salinity (Steele et al., 2005). In addition, both the rectal gland and gill exhibited changes in proteins involved in the inositol metabolism pathway (rectal gland: ALDH6A1 \uparrow 50% SW; gill: ALDOA \downarrow). Myoinositol may play a more prominent role in elasmobranch tissue osmoregulation than previously acknowledged (Steele et al., 2005; Yancey, 2001). The increase in ALDH6A1 in rectal gland is consistent with increased catabolism of β -alanine and/or myoinositol following salinity decrease in order to equilibrate intracellular osmolality with that of the plasma (and SW). Decreased abundance of PEPD in gill suggests reduced hydrolysis of proline-containing dipeptides (Tanoue et al., 1990), thus inhibiting accumulation of intracellular proline. Clearly further research on the interactions of intra- and extracellular osmolyte pools and the enzymes and transporters regulating their abundance is warranted in the context of elasmobranch euryhalinity.

Both tissues also exhibited overall decreases in proteins related to energy metabolism. Redirection of cellular energy supply is a classic component of the ‘cellular stress response’, during which processes that protect from and repair macromolecular damage increase at the expense of cell growth and proliferation (Kültz, 2003; Kültz, 2005). However, our data are more consistent with reduced energy/ATP requirements at lower salinity, particularly in rectal gland. Our proteomics data suggest decreased glycolytic flux in both rectal gland (GAPDH \downarrow 75% SW, PGAM2 \downarrow 50% SW) and gill (ALDOA \downarrow , opposite regulation of two GAPDH spots implying post-translational modifications). Further changes relevant to energy production were evident in rectal gland (TCA cycle, IDH2 \downarrow 50% SW; malate aspartate shuttle, MDH1 \downarrow 50% SW; oxidative phosphorylation, ATP5A1 mostly decreases 50% SW). The opposite pattern of regulation of two gill spots identified as PPA1 could also indicate modulation of oxidative phosphorylation due to PPA1’s role in phosphate metabolism and ATP synthesis. Interestingly, there were no significant changes in proteins directly associated with fuels other than glucose, despite the fact that ketones and/or fatty acids may be important energy sources in elasmobranch tissues (Ballantyne, 1997).

Our biochemical results indicate that decreased energy demand in rectal gland in 50% SW may be driven by reduced activity of the Na^+/K^+ -ATPase pump, whereas energy use in gill is probably not changing due to direct, organismal ionoregulatory functions. Interestingly, abundance of the ribosomal translation elongation factor EEF2 decreased significantly in leopard shark gill in 50% SW. Two proteins involved in the transcription of ribosomal RNAs also decreased in gill. Binding of the transcription factor UBTf to upstream promoters is necessary for ribosomal RNA expression (Grummt, 1999). TOP1 catalyzes the breaking and religation of bonds in the DNA backbone to relieve torsion caused

by transcription; it is concentrated in nucleoli, the sites of ribosomal DNA sequences (Leppard and Champoux, 2005). Given that ribosomal RNA translation constitutes 40–60% of translational activity (Hannan et al., 1998), these findings suggest a decrease in an energetically expensive process in gill during low salinity challenge. Similarly, in rectal gland we observed downregulation of several heterogeneous nuclear ribonucleoproteins, which regulate post-transcriptional processing and alternative splicing of mRNA (Martinez-Contreras et al., 2007), as well as PRPF4. These results possibly indicate a decrease from constitutive levels of transcription and protein synthesis in favor of stabilizing, repairing or degrading existing macromolecules (Kültz, 2005).

Proteasomal degradation and apoptosis

Although our proteomics data suggested responses related to proteasomal degradation of ubiquitinated proteins and cell death, especially in gill, our biochemical measurements of these processes revealed no effect of salinity. The 26S proteasome is an extremely large protein complex, and it is subject to complex regulatory networks (Adams, 2003; Ciechanover and Schwartz, 1998; Glickman and Raveh, 2005). Thus, although we found that several components of the proteasome were regulated by low salinity in gill, it is possible that these changes were insufficient to alter activity of the entire complex. In addition, our assay measured chymotrypsin-like activity but not the other two known proteolytic activities of the proteasome (caspase-like and trypsin-like). The non-ATPase PSMD12, which decreased in gill, is a component of the 19S regulatory lid that is necessary for organization and proper localization of the mature proteasome (Isono et al., 2007; Yen et al., 2003). PSMC2 (two spots decreased, one increased) also forms part of the 19S regulatory subunit, where it unfolds and deubiquitinates proteins prior to their degradation in the 20S proteasome core. We also observed a slight shift in the isoelectric points of two pairs of protein spots identified as proteasome subunit alpha type 2 on gill 2-D gels between 50% SW and 100% SW (Fig. 6). PSMA2 forms part of the 20S proteolytic core, where it regulates entry and exit of substrates (Bajorek and Glickman, 2004). Together, our biochemical and proteomic data implicate as yet unidentified post-translational modifications of these proteasome components, consistent with modulation of overall proteasome substrate specificity (Glickman and Raveh, 2005; Hartmann-Petersen and Gordon, 2004). The consequences of these salinity-induced modifications of proteasome constituents in leopard shark gill remain to be determined.

We found no evidence of changes in caspase 3/7 activity with salinity change in either tissue. We have also found no late apoptotic DNA degradation signal in leopard shark gill using a TUNEL assay (W.W.D., unpublished observations). These data differ from trends found in tilapia transferred from FW to SW, which exhibit a rapid (within 6h) and sustained increase in several measurements of apoptosis in gill (Kammerer and Kültz, 2009). Because partially euryhaline elasmobranchs appear to lack the tilapia's ability to remodel/turnover ionoregulatory epithelia to switch between ion excretion and ion absorption, apoptosis would be counterproductive for the organism in the short-term when behavioral avoidance is still possible and accumulated cellular damage is still relatively low. Rather, leopard shark cells appear to be activating acclimatory physiological mechanisms to solve the problems caused by low-salinity exposure. We know of no other data evaluating the role of apoptosis in osmoregulatory organs of elasmobranchs facing salinity change.

Cytoskeletal and membrane rearrangement within existing cells

Both gill and rectal gland exhibited consistent decreases in proteins associated with different components of the cytoskeleton. In rectal gland these included three keratins (all sequenced in elasmobranchs), which may indicate changes in cellular intermediate filament structure associated with the decrease in gland size. The rectal gland exhibits a surprising degree of morphological plasticity during gland activation after feeding (Matey et al., 2009). We hypothesize that analogous, but inverse, morphological reorganization operates in the rectal gland of leopard sharks exposed to decreasing salinity.

In gill, three proteins associated with the actin cytoskeleton decreased in abundance. EZR is a membrane-actin cytoskeleton crosslinker that prefers binding to ACTB (also decreased in gill) (Chen and Wagner, 2001). PLS3 belongs to a highly conserved family of actin bundling proteins (Delanote et al., 2005). ANXA4 (decreased in gill) belongs to a family of calcium-dependent, phospholipid-binding proteins. It associates with the apical membrane in epithelial cells, forms rigid 2-D arrays that may limit the mobility of integral membrane proteins (Piljic and Schultz, 2006), and inhibits epithelial calcium-dependent Cl^- secretion in colon cells (Xie et al., 1996). Overall, our proteomic and biochemical data implicate morphological changes within existing cells (possibly mediated by the proteasome), rather than cell turnover *via* apoptosis, in the leopard shark gill's response to salinity change.

How is the molecular response to salinity change coordinated?

Our proteomics analyses tended to identify effector proteins at the periphery of the IPA interaction networks, rather than the central sensor/initiator nodes, which tend to operate largely *via* post-translational signaling mechanisms that do not require changes in their abundance (Kültz, 2001a; Kültz, 2001b; Kültz and Avila, 2001). Along these lines, our pathway model for leopard shark rectal gland suggested a central role for 14-3-3 zeta (YWHAZ), a phosphoprotein adapter implicated in the adaptive osmoregulatory response in teleost gill (Kohn et al., 2003; Kültz et al., 2001). We know of no work on the function of 14-3-3 proteins in elasmobranchs.

Another intriguing result of our analysis is the presence of tumor necrosis factor α (TNF α) – a highly conserved, pleiotropic cytokine which also exhibits paracrine and autocrine activities – as a central node in the protein interaction networks of both rectal gland and gill. We hypothesize that TNF α is a key modulator of the osmoregulatory response in elasmobranch fishes. The effects of TNF α on ion and water balance may be mediated by salinity-dependent changes in the activity of the calcium-sensing receptor [implicated in elasmobranch salinity sensing (Nearing et al., 2002)] and/or the angiotensin II system [a major player in elasmobranch volume regulation (Anderson et al., 2006; Anderson et al., 2007)], as has been demonstrated in the mammalian kidney (Abdullah et al., 2006; Abdullah et al., 2008; Escalante et al., 1994; Ferreri et al., 1998; Ferreri et al., 1997). Binding of TNF α ligand can trigger apoptosis, activate gene transcription, stimulate amino acid uptake and/or have prosurvival (i.e. anti-apoptotic) effects (Dempsey et al., 2003; Inoue et al., 1995; Wajant et al., 2003). TNF α is also known to suppress the vault constituent MVP (decreased here in gill) (Stein et al., 1997). TNF α expression increased in salmonid gills around the parr-smolt transformation (Ingerslev et al., 2006), although the authors of this study did not relate this change to osmoregulatory adjustments. TNF α also factored in the hyperosmotic response network for tilapia gill cells

(Fiol et al., 2006), but again no mechanism for its action was postulated.

Do leopard sharks use behavior to offset or avoid physiological costs of salinity change in estuaries?

In scenarios where an environmental challenge nears or exceeds physiological plasticity, we would predict an important role for behavior in mitigating or avoiding potential physiological costs (Breuner and Hahn, 2003; Kidder, 1997; Schreck et al., 1997). 'Behavioral osmoregulation' in fishes could be driven by the energetic costs of osmoregulatory mechanisms (Kidder et al., 2006), and recent tracking studies have provided support for salinity-related movements in estuarine elasmobranchs (Heupel and Simpfendorfer, 2008; Ubeda et al., 2009). Bat Rays (*Myliobatis californica*) exhibited short-term doubling in organismal metabolic rate with salinity decrease (Meloni et al., 2002), and the organismal metabolic rate of leopard sharks doubled 1–2 h after transfer from 100% SW to 45% SW (C. Mull and J.C., Jr, unpublished observations). This energy may be more beneficially spent on moving out of the low-salinity conditions, especially if the longer-term consequences of exposure are even more severe. Even if leopard sharks suppress apoptotic pathways (as suggested by our data, although we cannot rule out apoptosis in other tissues or at other time points), the costs of coping with salinity change (e.g. *via* ATP-dependent proteasomal degradation) could be significant enough to trigger behavioral responses. Thus, we tentatively interpret the short-term increase in leopard shark swimming activity at low salinity as an attempted avoidance of physiologically challenging conditions. Long-term physiological costs could require sharks to reduce their activity when avoidance is not possible (as seen here), employing an 'evade, then survive' strategy.

The maintenance of urea concentrations in dilute salinity in the short-term preserved the massive gradient between the shark and the environment for urea loss while exacerbating the problem of osmotic water gain, documented here by the increase in muscle moisture. To maintain extracellular volume in dilute SW, renal glomerular filtration rate and urine flow rate increase manifold in elasmobranchs (Cooper and Morris, 2004; Goldstein and Forster, 1971; Janech et al., 2006; Janech and Piermarini, 2002). During the short-term, there may be high energetic costs of synthesizing urea [5 ATPs per urea molecule (Hochachka and Somero, 2002)] to replace that lost by diffusion and in the high volume of urine. Once 'committed' to a new osmotic equilibrium, longer-term adjustments in urea production and transport could include decreased expression of renal urea transporters (Morgan et al., 2003) and/or increased renal urea clearance (Goldstein and Forster, 1971). Interestingly, leopard shark kidney Na⁺/K⁺-ATPase activity did not change significantly with reduced salinity after 24 h but it doubled in sharks in 50–60% SW at 3 weeks relative to 100% SW controls. Whether this pattern of enzyme activity relates to delayed changes in renal urea reabsorption (*via* secondary active transport or an as yet undetected Na⁺/urea cotransporter, McDonald et al., 2006) remains to be determined.

Given the apparent lags in leopard sharks' physiological compensation for salinity change, why do partially euryhaline sharks inhabit estuaries at all? More work is needed to fully answer this question, including determining the frequency and severity of salinity changes experienced by sharks in the wild. If leopard sharks enter low salinity areas only for relatively short periods to feed or to avoid predation, then our physiological measurements would imply that urea concentrations and Na⁺/K⁺-ATPase activities are largely maintained over the short-term for subsequent re-entry into

seawater conditions. Recently, Ubeda et al. showed that bonnetheads (*Sphyrna tiburo*) move out of low salinity areas within a few days after salinity decreases (Ubeda et al., 2009). Should we find that leopard sharks occupy low and/or variable salinity conditions for extended periods in the wild, it would argue strongly for benefits such as food availability and predator avoidance outweighing the physiological costs of inhabiting dynamic estuarine habitats.

LIST OF ABBREVIATIONS

| | |
|----------------------|--------------------------------|
| BCA | bicinchoninic acid |
| CID | collision-induced dissociation |
| FW | freshwater |
| GO | gene ontology |
| HCT | hematocrit |
| IPA | Ingenuity Pathways Analysis |
| MCV | mean corpuscular volume |
| <i>M_r</i> | molecular mass |
| MS | mass spectrometry |
| pI | isoelectric point |
| PSD | post-source decay |
| RBC | red blood cells |
| SW | seawater |
| TCA | trichloroacetic acid |
| TFA | trifluoroacetic acid |

ACKNOWLEDGEMENTS

We acknowledge the support of the many people at Bodega Marine Laboratory (BML) who shared their laboratories and expertise. Greg Soyster, Stacey Fong, and Michelle Dulake assisted with experiments and laboratory analyses. Bob Kaufman, Heather Watts, and William Jewell (UC Davis Campus Mass Spectrometry Facility) provided technical assistance and numerous suggestions. This work was supported by several grants to W.W.D.: NSF Doctoral Dissertation Improvement Grant IOS-0709556, a Coastal Environmental Quality Initiative Fellowship from the UC Marine Council, a Mildred E. Mathias Student Research Grant from the UC Reserve System, American Elasmobranch Society Student Research Awards, Bodega Marine Laboratory Intercampus Travel Grants, UC Davis Jastro-Shields Research Fellowships, a Marin Rod and Gun Club Scholarship, and a Stockton Sportsmen's Club Research Scholarship. B.N.H. was supported by the BML NSF REU program (DBI-0453251). Additional support came from UC Agriculture Experiment Station grant 3455H to J.J.C. and NSF grant IOS-0542755 to D.K.

REFERENCES

- Abdullah, H. I., Pedraza, P. L., Hao, S., Rodland, K. D., McGiff, J. C. and Ferreri, N. R. (2006). NFAT regulates calcium-sensing receptor-mediated TNF production. *Am. J. Physiol.* **290**, F1110-F1117.
- Abdullah, H. I., Pedraza, P. L., McGiff, J. C. and Ferreri, N. R. (2008). CaR activation increases TNF production by mTAL cells *via* a G_i-dependent mechanism. *Am. J. Physiol.* **294**, F345-F354.
- Adams, J. (2003). The proteasome: structure, function, and role in the cell. *Cancer Treat. Rev.* **29**, Suppl. 1, 3-9.
- Altmann, J. (1974). Observational study of behavior: sampling methods. *Behaviour* **49**, 227-267.
- Anderson, W. G., Good, J. P. and Hazon, N. (2002). Changes in chloride secretion rate and vascular perfusion in the rectal gland of the European lesser-spotted dogfish in response to environmental and hormonal stimuli. *J. Fish Biol.* **60**, 1580-1590.
- Anderson, W. G., Good, J. P., Pillans, R. D., Hazon, N. and Franklin, C. E. (2005). Hepatic urea biosynthesis in the euryhaline elasmobranch *Carcharhinus leucas*. *J. Exp. Zool.* **303A**, 917-921.
- Anderson, W. G., Pillans, R. D., Hyodo, S., Tsukada, T., Good, J. P., Takei, Y., Franklin, C. E. and Hazon, N. (2006). The effects of freshwater to seawater transfer on circulating levels of angiotensin II, C-type natriuretic peptide and arginine vasotocin in the euryhaline elasmobranch, *Carcharhinus leucas*. *Gen. Comp. Endocrinol.* **147**, 39-46.
- Anderson, W. G., Taylor, J. R., Good, J. P., Hazon, N. and Grosell, M. (2007). Body fluid volume regulation in elasmobranch fish. *Comp. Biochem. Physiol.* **148A**, 3-13.
- Bajorek, M. and Glickman, M. H. (2006). Proteasome regulatory particles: keepers of the gates. *Cell. Mol. Life Sci.* **61**, 1579-1588.
- Ballantyne, J. S. (1997). Jaws: the inside story. The metabolism of elasmobranch fishes. *Comp. Biochem. Physiol.* **118B**, 703-742.
- Branstetter, S. (1990). Early life-history implications of selected carcharhinoid and lamnoid sharks of the Northwest Atlantic. *NOAA Tech. Rep. NMFS* **90**, 17-28.
- Breuner, C. W. and Hahn, T. P. (2003). Integrating stress physiology, environmental change, and behavior in free-living sparrows. *Horm. Behav.* **43**, 115-123.
- Calvano, S., Xiao, W., Richards, D., Felciano, R., Baker, H., Cho, R., Chen, R., Brownstein, B., Cobb, J., Tschoeke, S. et al. (2005). A network-based analysis of systemic inflammation in humans. *Nature* **437**, 1032-1037.

- Chen, J. and Wagner, M. C. (2001). Altered membrane-cytoskeleton linkage and membrane blebbing in energy-depleted renal proximal tubular cells. *Am. J. Physiol.* **280**, F619-F627.
- Ciechanover, A. and Schwartz, A. L. (1998). The ubiquitin-proteasome pathway: The complexity and myriad functions of proteins death. *Proc. Natl. Acad. Sci. USA* **95**, 2727-2730.
- Cooper, A. R. and Morris, S. (1998). Osmotic, ionic and haematological response of the Port Jackson shark *Heterodontus portusjacksoni* and the common stingaree *Trygonoptera testacea* upon exposure to diluted seawater. *Mar. Biol.* **132**, 29-42.
- Cooper, A. R. and Morris, S. (2004). Osmotic, sodium, carbon dioxide and acid-base state of the Port Jackson shark, *Heterodontus portusjacksoni*, in response to lowered salinity. *J. Comp. Physiol.* **174B**, 211-222.
- Delanote, V., Vandekerckhove, J. and Gettemans, J. (2005). Plastins: versatile modulators of actin organization in (patho)physiological cellular processes. *Acta Pharmacol. Sin.* **26**, 769-779.
- Dempsey, P. W., Doyle, S. E., He, J. Q. and Cheng, G. (2003). The signaling adaptors and pathways activated by TNF superfamily. *Cytokine Growth Factor Rev.* **14**, 193-209.
- Dowd, W. W., Wood, C. M., Kajimura, M., Walsh, P. J. and Kültz, D. (2008). Natural feeding influences protein expression in the dogfish shark rectal gland: a proteomic analysis. *Comp. Biochem. Physiol.* **3D**, 118-127.
- Escalante, B. A., Ferreri, N. R., Dunn, C. E. and McGiff, J. C. (1994). Cytokines affect ion transport in primary cultured thick ascending limb of Henle's loop cells. *Am. J. Physiol.* **266**, C1568-C1576.
- Evans, D. H., Piermarini, P. M. and Choe, K. P. (2004). Homeostasis: osmoregulation, pH regulation, and nitrogen excretion. In *Biology of Sharks and Their Relatives* (ed J. C. Carrier, J. A. Musick and M. R. Heithaus), pp. 247-268. Boca Raton, FL: CRC Press.
- Ferreri, N. R., Zhao, Y., Takizawa, H. and McGiff, J. C. (1997). Tumor necrosis factor- α -angiotensin interactions and regulation of blood pressure. *J. Hypertens.* **15**, 1481-1484.
- Ferreri, N. R., Escalante, B. A., Zhao, Y., An, S. J. and McGiff, J. C. (1998). Angiotensin II induces TNF production by the thick ascending limb: functional implications. *Am. J. Physiol.* **274**, F148-F155.
- Fines, G. A., Ballantyne, J. S. and Wright, P. A. (2001). Active urea transport and an unusual basolateral membrane composition in the gills of a marine elasmobranch. *Am. J. Physiol.* **280**, R16-R24.
- Fiol, D. F., Chan, S. Y. and Kültz, D. (2006). Identification and pathway analysis of immediate hyperosmotic stress responsive molecular mechanisms in tilapia (*Oreochromis mossambicus*) gill. *Comp. Biochem. Physiol.* **1D**, 344-356.
- Glickman, M. H. and Raveh, D. (2005). Proteasome plasticity. *FEBS Letts* **579**, 3214-3223.
- Goldstein, L. and Forster, R. P. (1971). Osmoregulation and urea metabolism in the little skate *Raja erinacea*. *Am. J. Physiol.* **220**, 742-746.
- Grummt, I. (1999). Regulation of mammalian ribosomal gene transcription by RNA polymerase I. *Prog. Nucleic Acid Res. Mol. Biol.* **62**, 109-154.
- Hannan, K. M., Hannan, R. D. and Rothblum, L. I. (1998). Transcription by RNA polymerase I. *Front. Biosci.* **3**, d376-d398.
- Hartmann-Petersen, R. and Gordon, C. (2004). Protein degradation: Recognition of ubiquitylated substrates. *Curr. Biol.* **14**, R754-R756.
- Hazon, N., Wells, A., Pillans, R. D., Good, J. P., Anderson, W. G. and Franklin, C. E. (2003). Urea based osmoregulation and endocrine control in elasmobranch fish with special reference to euryhalinity. *Comp. Biochem. Physiol.* **136B**, 685-700.
- Heupel, M. R. and Simpfendorfer, C. A. (2008). Movement and distribution of young bull sharks *Carcharhinus leucas* in a variable estuarine environment. *Aquat. Biol.* **1**, 277-289.
- Heupel, M. R., Carlson, J. K. and Simpfendorfer, C. A. (2007). Shark nursery areas: concepts, definition, characterization and assumptions. *Mar. Ecol. Progr. Ser.* **337**, 287-297.
- Hochachka, P. W. and Somero, G. N. (2002). Biochemical adaptation: mechanism and process in physiological evolution. New York, NY: Oxford University Press.
- Hopkins, T. E. and Cech, J. J., Jr (1995). Temperature effects on blood-oxygen equilibria in relation to movements of the bat ray, *Myliobatis californica* in Tomales Bay, California. *Mar. Behav. Physiol.* **24**, 227-235.
- Ingerslev, H. C., Cunningham, C. and Wergeland, H. I. (2006). Cloning and expression of TNF- α , IL-1 β and COX-2 in an anadromous and landlocked strain of Atlantic salmon (*Salmo salar* L.) during the smolting period. *Fish Shellfish Immunol.* **20**, 450-461.
- Inoue, Y., Bode, B. P., Copeland, E. M. and Souba, W. W. (1995). Enhanced hepatic amino acid transport in tumor-bearing rats is partially blocked by antibody to tumor necrosis factor. *Cancer Res.* **55**, 3525-3530.
- Isono, E., Nishihara, K., Saeki, Y., Yashiroda, H., Kamata, N., Ge, L., Ueda, T., Kikuchi, Y., Tanaka, K., Nakano, A. et al. (2007). The assembly pathway of the 19S regulatory particle of the yeast 26S proteasome. *Mol. Biol. Cell* **18**, 569-580.
- Janech, M. G. and Piermarini, P. M. (2002). Renal water and solute excretion in the Atlantic stingray in fresh water. *J. Fish Biol.* **61**, 1053-1057.
- Janech, M. G., Fitzgibbon, W. R., Ploth, D. W., Lacy, E. R. and Miller, D. H. (2006). Effect of low environmental salinity on plasma composition and renal function of the Atlantic stingray, a euryhaline elasmobranch. *Am. J. Physiol.* **291**, F770-F780.
- Kammerer, B. D. and Kültz, D. (2009). Prolonged apoptosis in mitochondria-rich cells of tilapia (*Oreochromis mossambicus*) exposed to elevated salinity. *J. Comp. Physiol.* **179B**, 535-542.
- Kidder, G. W., III (1997). Behavioral osmoregulation in *Fundulus heteroclitus*. *Bull. MDIBL* **36**, 69.
- Kidder, G. W., Petersen, C. W. and Preston, R. L. (2006). Energetics of osmoregulation: II. Water flux and osmoregulatory work in the euryhaline fish, *Fundulus heteroclitus*. *J. Exp. Zool.* **305A**, 318-327.
- Kohn, A., Chakravarty, D. and Kültz, D. (2003). Teleost Fh14-3-3a protein protects *Xenopus* oocytes from hyperosmolality. *J. Exp. Zool.* **299**, 103-109.
- Kültz, D. (2001a). Cellular osmoregulation: Beyond ion transport and cell volume. *Zoology* **104**, 198-208.
- Kültz, D. (2001b). Evolution of osmosensory MAP kinase signaling pathways. *Am. Zool.* **41**, 743-757.
- Kültz, D. (2003). Evolution of the cellular stress proteome: From monophyletic origin to ubiquitous function. *J. Exp. Biol.* **206**, 3119-3124.
- Kültz, D. (2005). Molecular and evolutionary basis of the cellular stress response. *Annu. Rev. Physiol.* **67**, 225-257.
- Kültz, D. and Avila, K. (2001). Mitogen-activated protein kinases are in vivo transducers of osmosensory signals in fish gill cells. *Comp. Biochem. Physiol.* **129B**, 821-829.
- Kültz, D., Chakravarty, D. and Adilakshmi, T. (2001). A novel 14-3-3 gene is osmoregulated in gill epithelium of the euryhaline teleost *Fundulus heteroclitus*. *J. Exp. Biol.* **204**, 2975-2985.
- Kültz, D., Fiol, D., Valkova, N., Gomez-Jimenez, S., Chan, S. Y. and Lee, J. (2007). Functional genomics and proteomics of the cellular osmotic stress response in 'non-model' organisms. *J. Exp. Biol.* **210**, 1593-1601.
- Lee, J., Valkova, N., White, M. P. and Kültz, D. (2006). Proteomic identification of processes and pathways characteristic of osmoregulatory tissues in spiny dogfish shark (*Squalus acanthias*). *Comp. Biochem. Physiol.* **1D**, 328-343.
- Leppard, J. B. and Champoux, J. J. (2005). Human DNA topoisomerase I: relaxation, roles, and damage control. *Chromosoma* **114**, 75-85.
- Lowe, C. G. (1996). Kinematics and critical swimming speed of juvenile scalloped hammerhead sharks. *J. Exp. Biol.* **199**, 2605-2610.
- Ma, B., Zhang, K., Hendrie, C., Liang, C., Li, M., Doherty-Kirby, A. and Lajoie, G. (2003). PEAKS: Powerful software for peptide de novo sequencing by tandem mass spectrometry. *Rapid Commun. Mass Spectrom.* **17**, 2337-2342.
- Martinez-Contreras, R., Cloutier, J. F., Shkreta, L., Fiset, J. F., Revil, T. and Chabot, B. (2007). hnRNP proteins and splicing control. *Adv. Exp. Med. Biol.* **623**, 123-147.
- Matey, V., Wood, C. M., Dowd, W. W., Kültz, D. and Walsh, P. J. (2009). Morphology of the rectal gland of the spiny dogfish (*Squalus acanthias*) shark in response to feeding. *Can. J. Zool.* **87**, 440-452.
- McCormick, S. D. (1993). Methods for nonlethal gill biopsy and measurement of Na⁺, K⁺-ATPase activity. *Can. J. Fish. Aquat. Sci.* **50**, 656-658.
- McDonald, M. D., Smith, C. P. and Walsh, P. J. (2006). The physiology and evolution of urea transport in fishes. *J. Membr. Biol.* **212**, 93-107.
- Meloni, C. J., Cech, J. J., Jr and Katzman, S. M. (2002). Effect of brackish salinities on oxygen consumption of bat rays (*Myliobatis californica*). *Copeia* **2002**, 462-465.
- Morgan, R. L., Ballantyne, J. S. and Wright, P. A. (2003). Regulation of a renal urea transporter with reduced salinity in a marine elasmobranch, *Raja erinacea*. *J. Exp. Biol.* **206**, 3285-3292.
- Nearing, J., Betka, M., Quinn, S., Hentschel, H., Elger, M., Baum, M., Bai, M., Chattopadhyay, N., Brown, E. M., Hebert, S. C. et al. (2002). Polyvalent cation receptor proteins (CaRs) are salinity sensors in fish. *Proc. Natl. Acad. Sci. USA* **99**, 9231-9236.
- Perkins, D. N., Pappin, D. J. C., Creasy, D. M. and Cottrell, J. S. (1999). Probability-based protein identification by searching sequence databases using mass spectrometry data. *Electrophoresis* **20**, 3551-3567.
- Piermarini, P. M. and Evans, D. H. (2000). Effects of environmental salinity on Na⁺/K⁺-ATPase in the gills and rectal gland of a euryhaline elasmobranch (*Dasyatis sabina*). *J. Exp. Biol.* **203**, 2957-2966.
- Piljic, A. and Schultz, C. (2006). Annexin A4 self-association modulates general membrane protein mobility in living cells. *Mol. Biol. Cell* **17**, 3318-3328.
- Pillans, R. D. and Franklin, C. E. (2004). Plasma osmolyte concentrations and rectal gland mass of bull sharks *Carcharhinus leucas*, captured along a salinity gradient. *Comp. Biochem. Physiol.* **138A**, 363-371.
- Pillans, R. D., Good, J. P., Anderson, W. G., Hazon, N. and Franklin, C. E. (2005). Freshwater to seawater acclimation of juvenile bull sharks (*Carcharhinus leucas*): plasma osmolytes and Na⁺/K⁺-ATPase activity in gill, rectal gland, kidney and intestine. *J. Comp. Physiol.* **175B**, 37-44.
- Schreck, C. B., Olla, B. L. and Davis, M. W. (1997). Behavioral responses to stress. In *Fish Stress and Health in Aquaculture* (ed G. K. Iwama, A. D. Pickering, J. P. Sumpter and C. B. Schreck), pp. 145-170. Cambridge: Cambridge University Press.
- Shevchenko, A., Sunyaev, S., Loboda, A., Shevchenko, A., Bork, P., Ens, W. and Standing, K. G. (2001). Charting the proteomes of organisms with unsequenced genomes by MALDI-quadrupole time-of-flight mass spectrometry and BLAST homology searching. *Anal. Chem.* **73**, 1917-1926.
- Springer, S. (1967). Social organization of shark populations. In *Sharks, Skates, and Rays* (ed P. W. Gilbert, R. F. Mathewson and D. P. Rall), pp. 111-140. Baltimore, MD: The Johns Hopkins University Press.
- Steele, S. L., Yancey, P. H. and Wright, P. A. (2005). The little skate *Raja erinacea* exhibits an extrahepatic ornithine urea cycle in the muscle and modulates nitrogen metabolism during low-salinity challenge. *Physiol. Biochem. Zool.* **78**, 216-226.
- Stein, U., Walther, W., Laurentot, C. M., Scheffer, G. L., Scheper, R. J. and Shoemaker, R. H. (1997). Tumor necrosis factor- α and expression of the multidrug resistance-associated genes LRP and MRP. *J. Natl. Cancer Inst.* **89**, 807-813.
- Sulikowski, J. A., Treberg, J. R. and Howell, W. H. (2003). Fluid regulation and physiological adjustments in the winter skate, *Leucoraja ocellata*, following exposure to reduced environmental salinities. *Environ. Biol. Fish.* **66**, 339-348.
- Tanoue, A., Endo, F. and Matsuda, I. (1990). Structural organization of the gene for human prolidase (peptidase D) and demonstration of a partial gene deletion in a patient with prolidase deficiency. *J. Biol. Chem.* **265**, 11306-11311.
- Ubeda, A. J., Simpfendorfer, C. A. and Heupel, M. R. (2009). Movements of bonnetheads, *Sphyrna tiburo*, as a response to salinity change in a Florida estuary. *Environ. Biol. Fish.* **84**, 293-303.
- Valkova, N., Yunis, R., Mak, S., Kang, K. and Kültz, D. (2005). Nek8 mutation causes overexpression of galectin-1, sorcin, and vimentin and accumulation of the major urinary protein in renal cysts of jck mice. *Mol. Cell. Proteomics* **4**, 1009-1018.

- Wajant, H., Pfizenmaier, K. and Scheurich, P.** (2003). Tumor necrosis factor signaling. *Cell Death Differ.* **10**, 45-65.
- Wood, C. M., Pärt, P. and Wright, P. A.** (1995). Ammonia and urea metabolism in relation to gill function and acid-base balance in a marine elasmobranch, the spiny dogfish (*Squalus acanthias*). *J. Exp. Biol.* **198**, 1545-1558.
- Xie, W., Kaetzel, M. A., Bruzik, K. S., Dedman, J. R., Shears, S. B. and Nelson, D. J.** (1996). Inositol 3,4,5,6-tetrakisphosphate inhibits the calmodulin-dependent protein kinase II-activated chloride conductance in T84 colonic epithelial cells. *J. Biol. Chem.* **271**, 14092-14097.
- Yancey, P. H.** (2001). Water stress, osmolytes and proteins. *Am. Zool.* **41**, 699-709.
- Yancey, P. H. and Somero, G. N.** (1978). Urea requiring lactate dehydrogenases of marine elasmobranch fishes. *J. Comp. Phys.* **125B**, 135-142.
- Yen, H. C., Espiritu, C. and Chang, E. C.** (2003). Rpn5 is a conserved proteasome subunit and required for proper proteasome localization and assembly. *J. Biol. Chem.* **278**, 30669-30676.
- Zeidel, J. D., Mathai, J. C., Campbell, J. D., Ruiz, W. G., Apodaca, G. L., Riordan, J. R. and Zeidel, M. L.** (2005). Selective permeability barrier to urea in shark rectal gland. *Am. J. Physiol.* **289F**, 72-82.